



MINISTRY OF DEFENCE (PROCUREMENT EXECUTIVE)

AERONAUTICAL RESEARCH COUNCIL

REPORTS AND MEMORANDA

# Numerical Solutions of Oscillatory Lift Interference

By K. R. RUSHTON and LUCY M. TOMLINSON

Dept. of Civil Engineering, University of Birmingham

## Part I—Oscillatory Lift Interference in Low-Speed Rectangular Tunnels with Porous-Slotted Roof and Floor

## Part II—Oscillatory Lift Interference in Subsonic Compressible Flow

LONDON: HER MAJESTY'S STATIONERY OFFICE

1972

£1.75 NET

# Numerical Solutions of Oscillatory Lift Interference

By K. R. RUSHTON and LUCY M. TOMLINSON

Dept. of Civil Engineering, University of Birmingham

---

*Reports and Memoranda No. 3700\**  
*May, 1971*

---

## Part I—Oscillatory Lift Interference in Low-Speed Rectangular Tunnels with Porous-Slotted Roof and Floor

### *Summary*

A solution of lift interference in oscillatory incompressible flow is described. Both steady and unsteady interference parameters are determined from a complete solution of the complex velocity potential, which is achieved by treating the real and imaginary parts separately throughout the tunnel, except at the tunnel walls where the two parts are linked through the boundary conditions. Both parts satisfy the Laplace equation which is solved using dynamic relaxation.

Results over a range of frequency are given for a square and a rectangular tunnel with different boundary conditions; the most involved being the porous-slotted boundary.

### CONTENTS

#### *Section*

1. Introduction
2. Interference Parameters
  - 2.1. Definitions
  - 2.2. Previous Solutions for Interference Parameters
    - 2.2.1. Direct Solution of Laplace Equation
3. Method of Solution
  - 3.1. Governing Differential Equations
  - 3.2. Small Wing
  - 3.3. Boundary Conditions

---

\* Replaces A.R.C. 31 615 and 32 822.

4. Numerical Solution
  - 4.1. Evaluation of  $\bar{\phi}_m$
  - 4.2. Zero Frequency
  - 4.3. Finite-Difference Solution
  - 4.4. Boundary Conditions
  - 4.5. Convergence
  - 4.6. Calculation of the Interference Parameters
  - 4.7. Finite Difference Error
  - 4.8. Estimated Accuracy
5. Results for Low Frequency
  - 5.1. The Integral for  $\delta'_0$
  - 5.2. Other Interference Parameters
6. Finite Frequency
7. Conclusions

Acknowledgements

List of Symbols

References

Tables 1 to 5

Illustrations—Figs. 1 to 9

## 1. Introduction

This report presents a general solution of the lift interference in oscillatory incompressible flow in slotted and perforated windtunnels. The differential equations governing the flow are written in finite-difference form and then solved numerically. Finite-difference studies of steady windtunnel interference have already been carried out using both an electrical analogue<sup>1, 2</sup> and the iterative method of dynamic relaxation;<sup>3</sup> which is now extended to general frequencies.

The major advance described in this report is achieved by considering the real and imaginary parts of the complex velocity potential separately, since both independently satisfy the Laplace equation in incompressible flow. However, both the real and imaginary parts of the function are involved in the application of boundary conditions on the walls of the tunnel; this presents complications, particularly in the case of the porous-slotted boundary.

Since this is a three-dimensional problem with complex boundary conditions requiring that the real and imaginary parts are solved simultaneously, there are difficulties in obtaining accurate solutions by dynamic relaxation on a digital computer. The finite-difference mesh cannot be as detailed as is desirable due to limitations in storage, and care has to be taken to obtain rapid convergence of the iterations so that the running time on the computer is not excessive. The lack of detail in the mesh leads to certain errors in the calculated parameters, but these are consistent errors whose magnitude can be estimated.

Results are presented for the interference in a square tunnel with many different conditions on the roof and floor over a range of frequency. Interference parameters are also given for a rectangular tunnel with breadth to height ratio 2.6 corresponding to a small half-model in the National Physical Laboratory 24 cm. × 24 cm. (9½ in. × 9½ in.) tunnel with wide slots and variable porosity. Six interference parameters are quoted for each tunnel studied and the definitions of these parameters are considered in the next section.

## 2. Interference Parameters

### 2.1 Definitions

The complex interference upwash on the axis of a windtunnel, at a distance  $x$  downstream of the wing, in incompressible oscillatory flow is defined as:

$$\begin{aligned} \left(\frac{\partial \bar{\phi}_i}{\partial z}\right)_x &= \left(\frac{\partial \bar{\phi}_{iR}}{\partial z}\right)_x + i \left(\frac{\partial \bar{\phi}_{iI}}{\partial z}\right)_x \\ &= \frac{US\bar{C}_L}{hb} \left[ \left( \delta_0 + \delta_1 \frac{x}{h} + \delta_2 \left(\frac{x}{h}\right)^2 + \dots \right) + \frac{i\omega h}{U} \left( \delta'_0 + \delta'_1 \frac{x}{h} + \delta'_2 \left(\frac{x}{h}\right)^2 + \dots \right) \right] \end{aligned} \quad (1)$$

where  $h$  is the height of the tunnel,  $b$  its breadth and  $\omega$ , the angular frequency of oscillation. The definitions of  $U$ ,  $S$  and  $\bar{C}_L$  are in the notation.

Interference parameters at  $x=0$  are given by the real and imaginary parts of equation (1),

$$\begin{aligned} \delta_0 &= \frac{hb}{US\bar{C}_L} \left(\frac{\partial \bar{\phi}_{iR}}{\partial z}\right)_{x=0}, & \delta_1 &= \frac{h^2b}{US\bar{C}_L} \left(\frac{\partial^2 \bar{\phi}_{iR}}{\partial x \partial z}\right)_{x=0} \quad \text{and} \\ \delta_2 &= \frac{h^3b}{2US\bar{C}_L} \left(\frac{\partial^3 \bar{\phi}_{iR}}{\partial^2 x \partial z}\right)_{x=0}. \end{aligned} \quad (2)$$

$$\begin{aligned} \delta'_0 &= \frac{b}{S\bar{C}_L\omega} \left(\frac{\partial \bar{\phi}_{iI}}{\partial z}\right)_{x=0}, & \delta'_1 &= \frac{hb}{S\bar{C}_L\omega} \left(\frac{\partial^2 \bar{\phi}_{iI}}{\partial x \partial z}\right)_{x=0} \quad \text{and} \\ \delta'_2 &= \frac{h^2b}{2S\bar{C}_L\omega} \left(\frac{\partial^3 \bar{\phi}_{iI}}{\partial^2 x \partial z}\right)_{x=0}. \end{aligned} \quad (3)$$

Therefore, all the six interference parameters can be determined from a solution of the real and imaginary parts of the interference upwash and its derivatives at the origin.

## 2.2 Previous Solutions for Interference Parameters

The steady lift interference parameter,  $\delta_0$ , has been calculated for many different windtunnels with various boundaries. An investigation into interference in ideal slotted tunnels was made by Davis and Moore<sup>4</sup>. This work was extended to a study of porous-slotted tunnels by Holder<sup>5</sup>, who derived an equation for calculating  $\delta_0$  in rectangular tunnels for any value of slot parameter and porosity parameter. An extensive description of the determination of windtunnel interference correction is given in Ref. 6, where many equations are quoted for the steady parameter  $\delta_0$  and also for  $\delta_1$  whenever there is a complete image system. These special cases include rectangular tunnels with closed sides and open or closed roof and floor, representing the extreme limits of the present investigation.

Garner et al<sup>7</sup> have developed a method for calculating the unsteady parameter,  $\delta'_0$ , of equation (1) from a knowledge of the steady interference upwash along the axis of the tunnel. The relation between steady acceleration potential and unsteady velocity potential is used. This was shown by Goodman<sup>8</sup> to be

$$\bar{\phi}(x, y, z) = \int_{-\infty}^x \exp\left[\frac{i\omega(x' - x)}{U}\right] \frac{\partial \phi_0(x', y, z)}{\partial x'} dx', \quad (4)$$

where  $\phi_0$  is the velocity potential of a steady vortex doublet. It is shown in Ref. 7 that the relationship given in equation (4) can be used to derive an expression, to the first order in frequency, for the complex interference upwash, which in incompressible flow is:

$$\left(\frac{\partial \bar{\phi}_i}{\partial z}\right)_x = \frac{US\bar{C}_L}{bh} \left[ \left( \delta_0 + \frac{\delta_1 x}{h} \right) + \frac{i\omega h}{U} \left( \delta'_0 - \frac{\delta_0 x}{h} - \frac{\delta_1 x^2}{2h^2} \right) + 0 \left( \frac{x}{h} \right)^3 \right], \quad (5)$$

where

$$\delta'_0 = -\frac{1}{h} \int_{-\infty}^0 \delta(x') dx' \quad (6)$$

depends on the steady distribution of interference upwash ahead of the origin of lift.

However, the relation given in equation (4) only holds when the boundary conditions for the steady and unsteady problems are the same. Therefore  $\delta'_0$  cannot strictly be calculated from equation (6) for the case of perforated or porous-slotted tunnels, but it is of interest to determine how inaccurate the results from equation (6) would be. A comparison of equations (1) and (5) shows the further identities

$$\delta_2 = 0, \quad \delta'_1 = -\delta_0 \quad \text{and} \quad \delta'_2 = -\frac{1}{2}\delta_1, \quad (7)$$

which only apply to tunnels with closed, open or ideal-slotted boundaries and for small frequency.

A recent extension of the method of images has been used by Streather<sup>9</sup> to determine values of  $\delta_0$ ,  $\delta_1$  and  $\delta'_0$  in ideal slotted tunnels. However, the method has not yet been adapted to study any type of porous boundary.

**2.2.1. Direct solution of Laplace equation.** An alternative approach for the study of unsteady wind-tunnel interference involves a direct solution of the Laplace equation for the complex velocity potential. The interference potential over the whole field is obtained; from this interference parameters can be calculated. For example Lo<sup>10, 11</sup> has used the Point Matching method of solving the Laplace equation to determine  $\delta_0$  in slotted windtunnels.

A solution of the Laplace equation is also possible on a resistance network<sup>1,2</sup> since the finite difference form of the equation is analogous to Kirchoff's current equation. A three-dimensional electrical analogue has been used to determine  $\delta_0$  and  $\delta_1$  in windtunnels with many different boundaries including perforated and porous-slotted walls.

The finite-difference form of the Laplace equation can also be solved on a digital computer by dynamic relaxation<sup>3</sup> and the dynamic-relaxation method is used in the present study in preference to the electrical analogue method due to the ease with which boundary conditions can be enforced.

### 3. Method of Solution

#### 3.1 Governing Differential Equation

The basic equation for incompressible oscillatory flow is

$$\frac{\partial^2 \bar{\phi}}{\partial x^2} + \frac{\partial^2 \bar{\phi}}{\partial y^2} + \frac{\partial^2 \bar{\phi}}{\partial z^2} = 0.$$

This is the Laplace equation for the complex velocity potential,

$$\bar{\phi} = \bar{\phi}_R + i\bar{\phi}_I.$$

The real and imaginary parts satisfy the Laplace equation independently, hence,

$$\frac{\partial^2 \bar{\phi}_R}{\partial x^2} + \frac{\partial^2 \bar{\phi}_R}{\partial y^2} + \frac{\partial^2 \bar{\phi}_R}{\partial z^2} = 0$$

and

$$\frac{\partial^2 \bar{\phi}_I}{\partial x^2} + \frac{\partial^2 \bar{\phi}_I}{\partial y^2} + \frac{\partial^2 \bar{\phi}_I}{\partial z^2} = 0.$$

Therefore the flow field for oscillatory incompressible flow can be studied from two separate solutions of the Laplace equation.

#### 3.2 Small Wing

The velocity potential due to a small oscillating wing in unconstrained flow is

$$\bar{\phi}_m = \frac{US\bar{C}_L}{8\pi} \int_0^{\infty} \frac{z e^{-i\omega x'/U}}{[(x-x')^2 + y^2 + z^2]^{3/2}} dx',$$

with real and imaginary parts;

$$\bar{\phi}_{mR} = \frac{US\bar{C}_L}{8\pi} \int_0^{\infty} \frac{z \cos(\omega x'/U)}{[(x-x')^2 + y^2 + z^2]^{3/2}} dx' \quad (8)$$

and

$$\bar{\phi}_{mI} = -\frac{US\bar{C}_L}{8\pi} \int_0^{\infty} \frac{z \sin(\omega x'/U)}{[(x-x')^2 + y^2 + z^2]^{3/2}} dx'. \quad (9)$$

Thus equations (8) and (9) represent the distribution from an oscillating wing at large distances relative to the size of the wing.

### 3.3 Boundary Conditions

A variety of conditions can apply on the walls of a tunnel. The most complicated boundary, the porous-slotted wall, will be considered first.

The porous-slotted boundary in oscillatory flow is represented by the homogeneous condition suggested in equation (6) of Ref. 7; thus

$$\left(\frac{\partial}{\partial x} + \frac{i\omega}{U}\right)\left(\bar{\phi} + K \frac{\partial \bar{\phi}}{\partial n}\right) + \frac{1}{P} \frac{\partial \bar{\phi}}{\partial n} = 0 \quad (10)$$

where  $K$  is the slot parameter and the porosity is represented by a real parameter  $P$ . The real and imaginary parts of equation (10) are:—

$$\frac{1}{P} \frac{\partial \bar{\phi}_R}{\partial n} = -\frac{\partial \bar{\phi}_R}{\partial x} + \frac{\omega}{U} \bar{\phi}_I - K \left( \frac{\partial^2 \bar{\phi}_R}{\partial x \partial n} - \frac{\omega}{U} \frac{\partial \bar{\phi}_I}{\partial n} \right) \quad (11)$$

and

$$\frac{1}{P} \frac{\partial \bar{\phi}_I}{\partial n} = -\frac{\partial \bar{\phi}_I}{\partial x} - \frac{\omega}{U} \bar{\phi}_R - K \left( \frac{\partial^2 \bar{\phi}_I}{\partial x \partial n} + \frac{\omega}{U} \frac{\partial \bar{\phi}_R}{\partial n} \right). \quad (12)$$

It should be noted that each equation contains both  $\bar{\phi}_R$  and  $\bar{\phi}_I$ .

Certain simpler boundary conditions can apply; for a perforated wall where the slot parameter  $K=0$ , similar equations are obtained but without the terms in brackets. The real and imaginary parts are still connected. However, for an ideal slotted wall where

$1/P=0$ , the equations reduce to

$$\bar{\phi}_R + K \frac{\partial \bar{\phi}_R}{\partial n} = 0 \quad (13)$$

and

$$\bar{\phi}_I + K \frac{\partial \bar{\phi}_I}{\partial n} = 0. \quad (14)$$

In this instance the real and imaginary parts are independent.

Far upstream the condition is that

$$\frac{\partial \bar{\phi}_R}{\partial x} = \frac{\partial \bar{\phi}_I}{\partial x} = 0. \quad (15)$$

This condition is simple to apply. Downstream, however, the velocity potential is oscillating and a boundary condition is introduced by extending the tunnel to the positions where  $\bar{\phi}_{mR}$  and  $\bar{\phi}_{mI}$  are zero on the axis and setting  $\bar{\phi}_R$  or  $\bar{\phi}_I$  zero across the whole transverse planes. These planes are at a different distance from the origin for the real and imaginary parts.

## 4. Numerical Solution

This section outlines the computational procedure and explains certain points which are important to the numerical solution.

### 4.1 Evaluation of $\bar{\phi}_m$

Before an analysis of interference potential can begin, values of the unconstrained velocity potential  $\bar{\phi}_m$  must be calculated on the boundary and near to the origin. This requires the evaluation of infinite

integrals, equations (8) and (9). These integrals are evaluated using the trapezoidal rule with a step interval of

$$\begin{aligned} &0.00001 h \text{ for } 0 < x < 0.2h \\ &0.0001 h \text{ for } 0.2h < x < 1.2h \\ &0.001 h \text{ for } 1.2h < x < 11.2h \text{ and finally} \\ &0.01 h \text{ for } 11.2h < x < 211.2h. \end{aligned}$$

The evaluation of both  $\bar{\phi}_{mR}$  and  $\bar{\phi}_{mI}$  at 15 nodes on a single plane takes approximately 15 minutes on a KDF 9 computer.

## 4.2 Zero Frequency

Since interference parameters are usually quoted for a frequency tending to zero, numerical results for low frequency were first considered. It has been shown in Ref. 12 that the results for  $\omega h/U = 0.01$  are very close to those in the limit as  $\omega h/U$  tends to zero, the difference in  $\delta_0$  being not more than 0.00006 and the difference in  $\delta'_0$  not more than 0.0003.

## 4.3 Finite-difference Solution

The differential equations are solved by the finite-difference method. The technique of writing the three-dimensional Laplace equation in finite-difference form for graded networks is described in detail in Ref. 2. In the study of oscillatory flow the velocity potential is divided into its real and imaginary parts, so that two three-dimensional networks are required.

Solution of the finite-difference equations is achieved by dynamic relaxation, which in essence is an iterative method in which arbitrary acceleration and damping terms are added to the finite-difference form of the governing equations. These equations are solved on a digital computer using an explicit method; and provided that optimum values of the time increment and damping coefficient are used, rapid convergence to the correct solution of the finite-difference equations occurs. This method has been used to solve steady-flow problems<sup>3</sup> for which only the real part of the function occurs, but its extension to the simultaneous solution of the real and imaginary parts of the Laplace equation is straightforward.

Since the dynamic relaxation method has been described in detail in Ref. 3 for the study of steady flow, only the features which are different in the case of oscillatory flow will be discussed. These are illustrated in the flow chart, Fig. 1. Note should be taken of the fact that the real and imaginary parts can be treated separately except in the calculation of the fictitious boundary points. Thus the two parts have to be held in the computer simultaneously to permit the calculation of the fictitious boundary values at each iteration.

As the real and imaginary functions are calculated simultaneously, the size of the working store of the computer becomes a limitation. If there are  $N$  nodal points for the real function, then effectively  $5N$  storage locations are required for the calculation of the real part and a similar number for the imaginary part. Since the available store of variables in the KDF 9 is roughly 20000 locations, the number of nodes,  $N$  cannot exceed 2000.

A further restriction results from the amount of computer time used in the calculation. If a network of 2000 nodes is used, the total solution takes almost 1 hour on the KDF 9. Therefore the calculation is stopped at step (d) to check the convergence of the velocity potential; then if the residuals are sufficiently small the calculation of the interference potential is carried out.

## 4.4 Boundary Conditions

The porous-slotted boundary condition of equation (10) is written in finite-difference form in the following manner. The real part of the boundary condition is rearranged to give,

$$\frac{\partial \bar{\phi}_R}{\partial n} = -P \left[ \frac{\partial \bar{\phi}_R}{\partial x} + K \frac{\partial^2 \bar{\phi}_R}{\partial x \partial n} - \frac{\omega}{U} \left( \bar{\phi}_I + K \frac{\partial \bar{\phi}_I}{\partial n} \right) \right].$$

This equation is then written in finite-difference form to give the value of  $\bar{\phi}_R$  at the fictitious node 1 (see Fig. 2):

$$\begin{aligned} \bar{\phi}_{R1} = & \bar{\phi}_{R6} - 2P\Delta z [(\bar{\phi}_{R4} - \bar{\phi}_{R2})/2\Delta x + K(3\bar{\phi}_{R4} - 4\bar{\phi}_{R7} + \bar{\phi}_{R10} - 3\bar{\phi}_{R2} + \\ & + 4\bar{\phi}_{R5} - \bar{\phi}_{R8})/(4\Delta x\Delta y) - (\omega/U)(\bar{\phi}_{13} + K(3\bar{\phi}_{13} - 4\bar{\phi}_{16} + \bar{\phi}_{19})/2\Delta z)]. \end{aligned} \quad (16)$$

A similar equation can be obtained from equation (12) for  $\bar{\phi}_{I1}$ .

This equation is also used for the application of the perforated boundary condition by setting  $K=0$ . However with ideal slotted boundaries, for which  $1/P=0$ , the conditions given by equations (13) and (14) for the real and imaginary parts are independent and the boundary can be represented in the standard manner (see Ref. 3).

#### 4.5 Convergence

The dynamic relaxation method is an iterative method which requires the correct choice of certain parameters to achieve a rapid convergence to the correct solution of the finite-difference equations. For steady flow, Ref. 3, a technique was developed in which the convergence parameters were determined automatically, but as this requires additional computing time it was not used for the oscillatory flow problems.

In most cases there was little difficulty in determining time increment and damping factors to give a good solution to the finite-difference equations. It was found to be advantageous to set the parameter  $\omega h/U$  equal to zero for the first third of the total number of iterations. Then the required value of  $\omega h/U$  was introduced and a rapid convergence was achieved.

For the closed rectangular tunnel,  $b/h=2.6$ , the optimum convergence parameters were:

$$\begin{aligned} \text{Time increment} & = 0.04, \\ \text{Damping factor} & = 3.0 \\ \text{and Number of iterations} & = 200. \end{aligned}$$

The problem for which convergence presented serious difficulty was the rectangular tunnel having closed side walls and porous-slotted roof and floor with  $F=0.233$  and  $1/P=1.0$ .

In this case the convergence factors were:

$$\begin{aligned} \text{Time increment} & = 0.03, \\ \text{Damping factor} & = 4.8 \\ \text{and Number of iterations} & = 260. \end{aligned}$$

This solution was particularly sensitive to the damping factor. For values of  $1/P$  less than 0.7 a convergent solution could not be obtained; a similar effect was noted with the earlier work on steady flow, Ref. 2.

With each computer output the residuals are calculated to check whether a satisfactory solution to the finite-difference equations has been obtained. If the residuals are sufficiently small (Ref. 3) then a satisfactory solution of the finite-difference equations has been obtained. However, errors due to the finite difference approximations can still occur.

#### 4.6 Calculation of the Interference Parameters

The interference parameters are calculated by writing equations (2) and (3) in finite-difference form. By fitting a third order polynomial and recognizing that there is anti-symmetry about the plane  $z=0$ , an

equation for  $\partial\phi/\partial z$  at  $x=0, y=0, z=0$  is derived as :

$$\left(\frac{\partial\phi}{\partial z}\right)_0 = \frac{1}{6d}(8\phi_1 - \phi_2 - 7\phi_0), \quad (17)$$

where  $d$  is the mesh interval,

$\phi_1$  is  $\phi$  at  $x=0, y=0, z=d$ ,

$\phi_2$  is  $\phi$  at  $x=0, y=0, z=2d$ ,

and  $\phi_0$  is 0.

Equations for  $\delta_1$  and  $\delta'_1$  also involve the derivative of interference potential in the streamwise direction. When a polynomial is fitted,

$$\left(\frac{\partial^2\phi}{\partial x\partial z}\right)_0 = \frac{1}{3d}\left(2\left(\frac{\partial\phi}{\partial z}\right)_1 - 2\left(\frac{\partial\phi}{\partial z}\right)_{-1}\right) + \frac{1}{12d}\left(\left(\frac{\partial\phi}{\partial z}\right)_{-2} - \left(\frac{\partial\phi}{\partial z}\right)_2\right) \quad (18)$$

where 1 and  $-1$  signify points on the  $x$  axis at distance  $d$  and  $-d$  from the origin, and 2 and  $-2$  are at distance  $2d$  and  $-2d$  from the origin.

The parameters  $\delta_2$  and  $\delta'_2$  are calculated from the equations

$$\left(\frac{\partial^3\phi}{\partial x^2\partial z}\right)_0 = \frac{1}{d^2}\left(-\frac{5}{4}\left(\frac{\partial\phi}{\partial z}\right)_0 + \frac{2}{3}\left[\left(\frac{\partial\phi}{\partial z}\right)_1 + \left(\frac{\partial\phi}{\partial z}\right)_{-1}\right] - \frac{1}{24}\left[\left(\frac{\partial\phi}{\partial z}\right)_2 + \left(\frac{\partial\phi}{\partial z}\right)_{-2}\right]\right). \quad (19)$$

#### 4.7 Finite Difference Error

The size of the computer store limits the number of mesh nodes to  $7 \times 7 \times 21$  for the square tunnel. (Note that when the fictitious nodes are included there are nearly 2000 points). With only six mesh intervals representing the tunnel half-height, a significant finite difference error is certain to occur as demonstrated in Table 1. This Table refers to the square closed tunnel in steady flow and lists the values of  $\delta_0$  for a number of different mesh configurations.

Particular note should be taken of the lengths of the intervals adjacent to the tunnel axis and roof respectively. The first line of the Table refers to the mesh used in the present investigation, the other results are taken from Ref. 2.

From this Table it is clear that the limitation of using only six mesh intervals causes significant errors in the interference parameters. However, if a faster computer with a larger store was available, an increase in the number of mesh intervals would be obtained with a resultant decrease in the finite-difference errors.

#### 4.8 Estimated Accuracy

Two particular sources of error need to be considered :

- (1) Errors due to an inadequate finite-difference mesh,
- (2) Errors due to numerical differentiation whilst obtaining the interference parameters.

Significant errors do arise because it is not possible to use sufficient mesh intervals. Section 4.7 showed the effect for the square closed tunnel and similar discrepancies occur with other boundary conditions. For example, the results for  $\delta_0$  in a rectangular tunnel with porous-slotted walls obtained from a solution with the tunnel half-height represented by 6 mesh intervals, are compared in Fig. 3 with theoretical values of  $\delta_0^5$ .

It is important to note that the greatest errors occur for a tunnel with closed roof and floor. The reason is that the widely spaced mesh intervals adjacent to the roof and floor give a poor representation of the boundary condition,  $\partial\phi/\partial z=0$ .

Errors can also arise during numerical differentiation. However by using the five point formulae, equations (18) and (19), this effect can be minimised and the errors due to this cause are certainly far smaller than those arising from insufficient mesh intervals.

The maximum errors from both sources are estimated to be:

Square tunnel,

6 × 6 mesh intervals, maximum error in all parameters, 0.008,

Rectangular tunnel,

6 × 7 mesh intervals, maximum error in all parameters, 0.020.

In most instances the finite-difference results for  $\delta_0$ ,  $\delta_1$  and  $-\delta'_1$  are likely to be too high. These errors are consistent errors (not random errors, *see* Fig. 3) and are most serious with closed boundaries. For many other boundary conditions the errors are roughly half the values quoted above.

## 5. Results for Low Frequency

The results for low frequency are recorded in Tables 2 and 3. A value of frequency parameter,  $\omega h/U = 0.01$  is used; this gives results very close to those for a frequency parameter of zero.

Results are presented for a square tunnel ( $b/h = 1.0$ ) and for a rectangular tunnel ( $b/h = 2.6$ ), representing the N.P.L.  $9\frac{1}{2}$  in ×  $9\frac{1}{2}$  in (24 cm × 24 cm) tunnel with a half model. The non-dimensional slot parameter,  $F = 2K/h = 0.233$  is that corresponding to the experiments reported in Ref. 13.

For the rectangular tunnel ( $b/h = 2.6$ ) with a porous-slotted roof and floor, analytical values of  $\delta_0$  have been calculated from the equation given in Ref. 5. These values are plotted against those given by dynamic relaxation in Fig. 3.

It will be seen that the numerical errors decrease rapidly as  $1/P$  decreases. The greatest errors occur for the closed tunnel, while at the other extreme with open roof and floor,  $\bar{\phi}_i = -\bar{\phi}_m$  is prescribed on that boundary and in consequence the finite-difference error is minimized.

### 5.1 The Integral for $\delta'_0$

One important aspect of these results is that they demonstrate that serious errors arise if the integral of equation (6) is used to evaluate  $\delta'_0$  for porous tunnels. In Fig. 4 the true values of  $\delta'_0$  calculated from  $\partial\bar{\phi}_{ii}/\partial z$  according to equation (3) are plotted as full lines and are compared with the broken lines obtained by equation (6). A similar difference occurs between the true and integrated values for  $\delta'_0$  for both the square and rectangular tunnels with  $F=0$  and  $F=0.233$ .

Except for the end points where the boundary conditions are closed, open or ideal slotted, the results from the integral are seriously inconsistent. The true behaviour of  $\delta'_0$  against  $(1+1/P)^{-1}$  is in marked contrast to the more linear behaviour of  $\delta_0$ . The variation of  $\delta'_0$  with slot parameter  $(1+F)^{-1}$  for a fixed value  $1/P=3$  in the square tunnel is plotted in Fig. 5. Unlike the integral in equation (6), the true  $\delta'_0$  shows little dependence on slot parameter.

These results dispel any hope that for porous-slotted tunnels and low frequency the wall interference can be estimated from the distribution of interference upwash in steady flow. There is apparently no short cut to the present results.

### 5.2 Other Interference Parameters

Sufficient values are presented in Tables 2 and 3 to show how most of the interference parameters vary with the porosity parameter and the slot parameter; so only brief comment will be made on some of the results.

For the cases where the porosity parameter  $1/P$  is zero or infinity, the identities of equation (7) should hold. It will be noted from the results that for closed, open and ideal slotted tunnels

$$\begin{aligned}\delta'_1 &\simeq \delta_0, \\ \delta_2 &\simeq 0, \\ \text{and} \quad \delta'_2 &\simeq -\frac{1}{2}\delta_1.\end{aligned}$$

For  $1/P$  not equal to zero,  $\delta_2$  becomes large and positive.

Though these Tables only give the interference upwash and its derivatives at the origin of the tunnel, the dynamic relaxation solutions provide information about the interference at any point in the tunnel. For example, Figs. 6 and 7 show the variation in  $\delta$  and  $\delta'$  along the tunnel axis for the square tunnel with closed side walls and ideal slotted roof and floor. Fig. 8 shows a plot of  $\delta$  for the same tunnel with  $F=0$  and  $1/P$  taking various values. The curvature of  $\delta(x)$  at  $x=0$  is responsible for the large values of  $\delta_2$  where  $1/P$  is non-zero and finite.

## 6. Finite Frequency

Results have also been obtained to show how the interference changes with frequency. Only square tunnels are considered with closed side walls and either slotted or perforated roof and floor.

No special techniques are required to obtain computer solutions, though for a frequency parameter  $\omega h/U > 1.0$  the downstream boundaries are taken as the second planes at which  $\bar{\phi}_{mR}$  and  $\bar{\phi}_{mI}$  are zero.

The results for the interference parameters are presented in Tables 4 and 5 and the variations of  $\delta_0$  and  $\delta'_0$  with frequency for the slotted tunnel are plotted in Fig. 9. It can be seen from the Tables that the identities in equation (7) do not hold for a high frequency even when  $1/P$  is zero or infinity.

Fig. 9 shows how both parameters are tending towards zero as frequency parameter increases. Where  $\delta_0$  and  $\delta'_0$  are large for low  $\omega h/U$ , they decrease by a factor of order 4 for  $\omega h/U = 4$ .

## 7. Conclusions

This report has demonstrated that unsteady incompressible lift interference in rectangular tunnels can be analysed using the dynamic relaxation method. Numerous boundary conditions including the porous-slotted boundary have been included and a range of typical results are tabulated. Due to limitations in computer storage, finite difference errors have occurred, these could be reduced if a larger computer were available.

The results have verified that a method of calculating one of the unsteady interference parameters,  $\delta'_0$ , from the steady interference upwash, does not give true answers for the case of perforated or porous-slotted tunnels though it does give correct results for low frequency, ideal-slotted tunnels.

The technique is being developed to study the effect of oscillatory compressible flow in rectangular wind tunnels with the same range of boundary conditions and various frequency parameters.

## Acknowledgement

The authors wish to acknowledge the help given by Mr. H. C. Garner of the National Physical Laboratory with the theoretical aspect of the study.

## LIST OF SYMBOLS

|                                 |  |
|---------------------------------|--|
| $b$                             | Tunnel breadth   |
| $\bar{C}_L$                     | Complex lift/ $\frac{1}{2}\rho U^2 S$  |
| $F$                             | Non-dimensional slot parameter. $2K/h$   |
| $h$                             | Tunnel height  |
| $i$                             | $(-1)^{\frac{1}{2}}$   |
| $K$                             | Geometric slot parameter (defined in Ref. 7)   |
| $M$                             | Mach number of undisturbed stream  |
| $n$                             | Outward normal distance from boundary  |
| $P$                             | Porosity parameter   |
| $S$                             | Planform area of wing  |
| $U$                             | Velocity of undisturbed stream   |
| $x, y, z$                       | Cartesian coordinates  |
| $x'$                            | Increment in stream-wise direction   |
| $\beta$                         | $(1 - M^2)^{\frac{1}{2}}$  |
| $\delta, \delta'$               | Distribution of real and imaginary interference upwash along the axis of the tunnel    |
| $\delta_0 \delta_1 \delta_2$    | Steady interference parameters in equation (2)   |
| $\delta'_0 \delta'_1 \delta'_2$ | Unsteady interference parameters in equation (3)                                       |
| $\Delta$                        | Increment  |
| $\rho$                          | Density of undisturbed stream  |
| $\bar{\phi}$                    | Complex perturbation velocity potential, $\bar{\phi}_R + i\bar{\phi}_I$                |
| $\bar{\phi}_m$                  | Complex velocity potential in unconstrained flow, $\bar{\phi}_{mR} + i\bar{\phi}_{mI}$ |
| $\bar{\phi}_i$                  | Complex interference potential, $\bar{\phi}_{iR} + i\bar{\phi}_{iI}$                   |
| $\phi_0$                        | $\phi$ corresponding to steady horse-shoe vortex in incompressible flow                |
| $\omega$                        | Angular frequency of oscillation   |

## REFERENCES

- 1 K. R. Rushton .. .. Studies of slotted-wall interference using an electrical analogue.  
A.R.C. R. & M. No. 3452 (1965).
- 2 K. R. Rushton and .. .. A general method of studying steady lift interference in slotted and  
Lucy M. Laing perforated tunnels.  
A.R.C. R. & M. No. 3567 (1967).
- 3 K. R. Rushton and .. .. A digital computer solution of the Laplace equation using the  
Lucy M. Laing Dynamic Relaxation method.  
Aeron. Quart., Vol. XIX. Pt. 4. Nov. 1968, pp. 375–387.
- 4 D. D. Davis and D. Moore .. Analytical study of blockage- and lift-interference corrections for  
slotted tunnels obtained by the substitution of an equivalent  
homogeneous boundary for the discrete slots.  
NACA RM L53E076 (NACA/TIB/3792). June 1953.
- 5 D. R. Holder .. .. Upwash interference in a rectangular wind tunnel with closed  
side walls and porous slotted floor and roof.  
A.R.C. R. & M. No. 3322 (1962).
- 6 H. C. Garner .. .. Subsonic wind tunnel wall corrections.  
Agardograph 109, AGARD, Paris. 1966.
- 7 H. C. Garner, A. W. Moore .. The theory of interference effects on dynamic measurements in  
and K. C. Wight slotted-wall tunnels at subsonic speeds and comparisons with  
experiment.  
A.R.C. R. & M. No. 3500 (1966).
- 8 T. R. Goodman .. .. The upwash correction for an oscillating wing in a wind tunnel.  
J. Aero. Sci., Vol. 20, pp. 383–386, 406. 1953.
- 9 R. A. Streater .. .. Ventilated wall interference on large wind tunnel models in  
oscillating motion.  
Ph.D. Thesis. Southampton University. 1969.
- 10 C. F. Lo .. .. Method of calculating the wind tunnel interference for steady and  
oscillating wings in tunnels of arbitrary wall configuration.  
AEDC-TR-68-42. March 1968.
- 11 C. F. Lo .. .. A V/STOL wind tunnel wall interference study.  
AIAA Paper No. 69-171. January 1969.
- 12 K. R. Rushton and .. .. Finite difference solutions for an unsteady interference parameter  
Lucy M. Laing in slotted wind tunnels.  
A.R.C. C.P. No. 1053 (1968).
- 13 A. W. Moore and .. .. An experimental investigation of windtunnel wall conditions for  
K. C. Wight interference free dynamic measurements.  
N.P.L. Aero Report 1307. A.R.C. 31704 (1969).

TABLE 1

| No. of Mesh Sub-divisions<br>in half-height | Mesh interval adjacent<br>to origin | Mesh interval adjacent<br>to roof | $\delta_0$ |
|---|-------------------------------------|-----------------------------------|------------|
| 6   | 0.0417 $h$                          | 0.125 $h$                         | 0.145      |
| 7   | 0.04 $h$                            | 0.1 $h$                           | 0.138      |
| 8   | 0.03125 $h$                         | 0.125 $h$                         | 0.134      |
| 44  | 0.0114 $h$                          | 0.0114 $h$                        | 0.137      |
| Analytical                                  | —                                   | —                                 | 0.1368     |

TABLE 2

*Interference Parameters Square Tunnel Low Frequency.*

| ROOF & FLOOR   |          |               | $\delta_0$ | $\delta'_0$ | $\delta_1$ | $\delta'_1$ | $\delta_2$ | $\delta'_2$ |
|--|----------|---------------|------------|-------------|------------|-------------|------------|-------------|
| $\frac{\omega h}{U}$                                 | $F$      | $\frac{1}{P}$ |            |             |            |             |            |             |
| <i>Square <math>b/h=1.0</math> closed side walls</i> |          |               |            |             |            |             |            |             |
| 0.01   | $\infty$ | $\infty$      | 0.145      | -0.036      | 0.274      | -0.145      | 0.000      | -0.129      |
| 0.01   | 0        | 9.0           | 0.127      | -0.035      | 0.273      | -0.146      | 0.026      | -0.130      |
| 0.01   | 0        | 3.0           | 0.089      | -0.029      | 0.258      | -0.144      | 0.085      | -0.137      |
| 0.01   | 0        | 1.0           | 0.009      | 0.004       | 0.172      | -0.104      | 0.177      | -0.151      |
| 0.01   | 0        | 0.7           | -0.020     | 0.020       | 0.118      | -0.069      | 0.189      | -0.141      |
| 0.01   | 0        | 0             | -0.124     | 0.077       | -0.179     | 0.124       | 0.000      | 0.087       |
| 0.01   | 0.233    | 7.0           | 0.120      | -0.034      | 0.270      | -0.146      | 0.040      | -0.131      |
| 0.01   | 0.233    | 3.0           | 0.090      | -0.027      | 0.252      | -0.142      | 0.084      | -0.139      |
| 0.01   | 0.233    | 1.0           | 0.024      | 0.003       | 0.154      | -0.094      | 0.137      | -0.138      |
| 0.01   | 0.233    | 0             | -0.067     | 0.058       | -0.060     | 0.067       | 0.000      | 0.031       |
| 0.01   | 0.1      | 3.0           | 0.090      | -0.028      | 0.255      | -0.143      | 0.085      | -0.138      |
| 0.01   | 1.0      | 3.0           | 0.096      | -0.025      | 0.240      | -0.137      | 0.074      | -0.135      |

TABLE 3

*Interference Parameters Rectangular Tunnel Low Frequency.*

| ROOF & FLOOR                                 |          |               | $\delta_0$ | $\delta'_0$ | $\delta_1$ | $\delta'_1$ | $\delta_2$ | $\delta'_2$ |
|--|----------|---------------|------------|-------------|------------|-------------|------------|-------------|
| $\frac{\omega h}{U}$                         | $F$      | $\frac{1}{P}$ |            |             |            |             |            |             |
| <i>Rectangular b/h=2.6 closed side walls</i> |          |               |            |             |            |             |            |             |
| 0.01   | $\infty$ | $\infty$      | 0.191      | -0.005      | 0.444      | -0.191      | 0.000      | -0.205      |
| 0.01   | 0        | 7.0           | 0.148      | -0.003      | 0.440      | -0.194      | 0.078      | -0.210      |
| 0.01   | 0        | 3.0           | 0.091      | 0.006       | 0.416      | -0.189      | 0.175      | -0.221      |
| 0.01   | 0        | 1.0           | -0.060     | 0.061       | 0.255      | -0.125      | 0.378      | -0.255      |
| 0.01   | 0        | 0             | -0.342     | 0.205       | -0.507     | 0.342       | 0.000      | 0.247       |
| 0.01   | 0.233    | 7.0           | 0.148      | -0.003      | 0.437      | -0.194      | 0.083      | -0.211      |
| 0.01   | 0.233    | 3.0           | 0.093      | 0.009       | 0.404      | -0.188      | 0.176      | -0.224      |
| 0.01   | 0.233    | 1.5           | 0.018      | 0.037       | 0.317      | -0.152      | 0.268      | -0.240      |
| 0.01   | 0.233    | 1.0           | -0.033     | 0.062       | 0.232      | -0.103      | 0.293      | -0.228      |
| 0.01   | 0.233    | 0             | -0.215     | 0.165       | -0.233     | 0.215       | 0.000      | 0.118       |

TABLE 4

*Interference Parameters for Ideal Slotted Square Tunnel, Variable Frequency.*

| ROOF & FLOOR                           |          |               |            |             |            |             |            |             |
|--|----------|---------------|------------|-------------|------------|-------------|------------|-------------|
| $\frac{\omega h}{U}$                   | $F$      | $\frac{1}{P}$ | $\delta_0$ | $\delta'_0$ | $\delta_1$ | $\delta'_1$ | $\delta_2$ | $\delta'_2$ |
| <i>Square tunnel closed side walls</i> |          |               |            |             |            |             |            |             |
| 0.01                                   | $\infty$ | 0             | 0.144      | -0.036      | 0.274      | -0.145      | 0.000      | -0.129      |
| 0.01                                   | 3.0      | 0             | 0.084      | -0.005      | 0.188      | -0.086      | -0.004     | -0.090      |
| 0.01                                   | 1.0      | 0             | 0.019      | 0.024       | 0.090      | -0.018      | -0.003     | -0.039      |
| 0.01                                   | 0.3      | 0             | -0.055     | 0.053       | -0.036     | 0.054       | -0.001     | 0.020       |
| 0.01                                   | 0        | 0             | -0.124     | 0.076       | -0.175     | 0.124       | 0.000      | 0.086       |
| 0.1                                    | $\infty$ | 0             | 0.145      | -0.038      | 0.274      | -0.145      | -0.001     | -0.128      |
| 0.1                                    | 3.0      | 0             | 0.084      | -0.008      | 0.187      | -0.083      | 0.003      | -0.084      |
| 0.1                                    | 1.0      | 0             | 0.020      | 0.021       | 0.090      | -0.019      | -0.002     | -0.043      |
| 0.1                                    | 0.3      | 0             | -0.054     | 0.050       | -0.035     | 0.054       | 0.000      | 0.017       |
| 0.1                                    | 0        | 0             | -0.123     | 0.073       | -0.175     | 0.122       | 0.003      | 0.086       |
| 0.5                                    | $\infty$ | 0             | 0.145      | -0.046      | 0.262      | -0.145      | -0.118     | -0.123      |
| 0.5                                    | 3.0      | 0             | 0.083      | -0.017      | 0.212      | -0.087      | -0.109     | -0.084      |
| 0.5                                    | 1.0      | 0             | 0.021      | 0.011       | 0.121      | -0.026      | -0.101     | -0.042      |
| 0.5                                    | 0.3      | 0             | -0.050     | 0.039       | 0.003      | 0.045       | -0.090     | 0.014       |
| 0.5                                    | 0        | 0             | -0.117     | 0.062       | -0.131     | 0.111       | -0.079     | 0.078       |
| 1.0                                    | $\infty$ | 0             | 0.136      | -0.048      | 0.222      | -0.133      | -0.067     | -0.102      |
| 1.0                                    | 3.0      | 0             | 0.087      | -0.022      | 0.162      | -0.084      | -0.046     | -0.074      |
| 1.0                                    | 1.0      | 0             | 0.032      | 0.003       | 0.091      | -0.030      | -0.018     | -0.040      |
| 1.0                                    | 0.3      | 0             | -0.033     | 0.029       | -0.008     | 0.033       | 0.016      | 0.006       |
| 1.0                                    | 0        | 0             | -0.095     | 0.050       | -0.125     | 0.095       | 0.049      | 0.062       |
| 2.0                                    | $\infty$ | 0             | 0.099      | -0.039      | 0.107      | -0.095      | -0.187     | -0.045      |
| 2.0                                    | 3.0      | 0             | 0.069      | -0.022      | 0.091      | -0.064      | -0.130     | -0.038      |
| 2.0                                    | 1.0      | 0             | 0.034      | -0.004      | 0.065      | -0.031      | -0.064     | -0.028      |
| 2.0                                    | 0.3      | 0             | -0.012     | 0.015       | 0.020      | 0.012       | 0.023      | -0.008      |
| 2.0                                    | 0        | 0             | -0.060     | 0.032       | -0.050     | 0.059       | 0.118      | 0.023       |
| 4.0                                    | $\infty$ | 0             | 0.031      | -0.020      | -0.044     | -0.034      | -0.235     | 0.013       |
| 4.0                                    | 3.0      | 0             | 0.024      | -0.013      | -0.026     | -0.027      | -0.188     | 0.006       |
| 4.0                                    | 1.0      | 0             | 0.016      | -0.006      | -0.006     | -0.017      | -0.123     | -0.002      |
| 4.0                                    | 0.3      | 0             | 0.002      | 0.004       | 0.016      | -0.003      | -0.018     | -0.010      |
| 4.0                                    | 0        | 0             | -0.018     | 0.013       | 0.028      | 0.017       | 0.135      | -0.014      |

TABLE 5

*Interference Parameters for Perforated Tunnel, Variable Frequency.*

| ROOF & FLOOR                           |     |               | $\delta_0$ | $\delta'_0$ | $\delta_1$ | $\delta'_1$ | $\delta_2$ | $\delta'_2$ |
|--|-----|---------------|------------|-------------|------------|-------------|------------|-------------|
| $\frac{\omega h}{U}$                   | $F$ | $\frac{1}{P}$ |            |             |            |             |            |             |
| <i>Square tunnel closed side walls</i> |     |               |            |             |            |             |            |             |
| 0.01                                   | 0   | $\infty$      | 0.144      | -0.036      | 0.274      | -0.145      | 0.000      | -0.129      |
| 0.01                                   | 0   | 9.0           | 0.127      | -0.035      | 0.273      | -0.146      | 0.026      | -0.130      |
| 0.01                                   | 0   | 3.0           | 0.089      | -0.029      | 0.258      | -0.144      | -0.085     | -0.137      |
| 0.01                                   | 0   | 1.0           | 0.009      | 0.004       | 0.172      | -0.104      | 0.177      | -0.151      |
| 0.01                                   | 0   | 0             | -0.124     | 0.077       | -0.179     | 0.124       | 0.000      | 0.087       |
| 0.1                                    | 0   | $\infty$      | 0.145      | -0.038      | 0.274      | -0.145      | -0.001     | -0.128      |
| 0.1                                    | 0   | 9.0           | 0.126      | -0.037      | 0.272      | -0.146      | 0.029      | -0.129      |
| 0.1                                    | 0   | 3.0           | 0.090      | -0.031      | 0.257      | -0.144      | 0.085      | -0.136      |
| 0.1                                    | 0   | 1.0           | 0.010      | 0.001       | 0.172      | -0.104      | 0.176      | -0.151      |
| 0.1                                    | 0   | 0             | -0.123     | 0.073       | -0.175     | 0.122       | 0.003      | 0.086       |
| 0.5                                    | 0   | $\infty$      | 0.145      | -0.046      | 0.262      | -0.145      | -0.118     | -0.123      |
| 0.5                                    | 0   | 9.0           | 0.126      | -0.045      | 0.260      | -0.146      | 0.012      | -0.135      |
| 0.5                                    | 0   | 3.0           | 0.090      | -0.039      | 0.245      | -0.145      | 0.067      | -0.131      |
| 0.5                                    | 0   | 1.0           | 0.013      | -0.007      | 0.163      | -0.109      | 0.158      | -0.146      |
| 0.5                                    | 0   | 0             | -0.117     | 0.062       | -0.131     | 0.111       | -0.079     | 0.078       |
| 1.0                                    | 0   | $\infty$      | 0.136      | -0.048      | 0.222      | -0.133      | -0.067     | -0.102      |
| 1.0                                    | 0   | 9.0           | 0.117      | -0.047      | 0.220      | -0.134      | -0.037     | -0.103      |
| 1.0                                    | 0   | 3.0           | 0.082      | -0.041      | 0.206      | -0.133      | 0.018      | -0.110      |
| 1.0                                    | 0   | 1.0           | 0.012      | -0.012      | 0.267      | -0.098      | 0.108      | -0.127      |
| 1.0                                    | 0   | 0             | -0.095     | 0.050       | -0.125     | 0.095       | 0.049      | 0.062       |



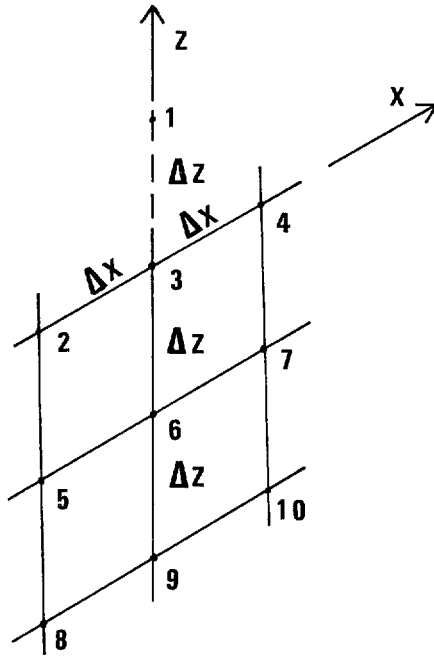
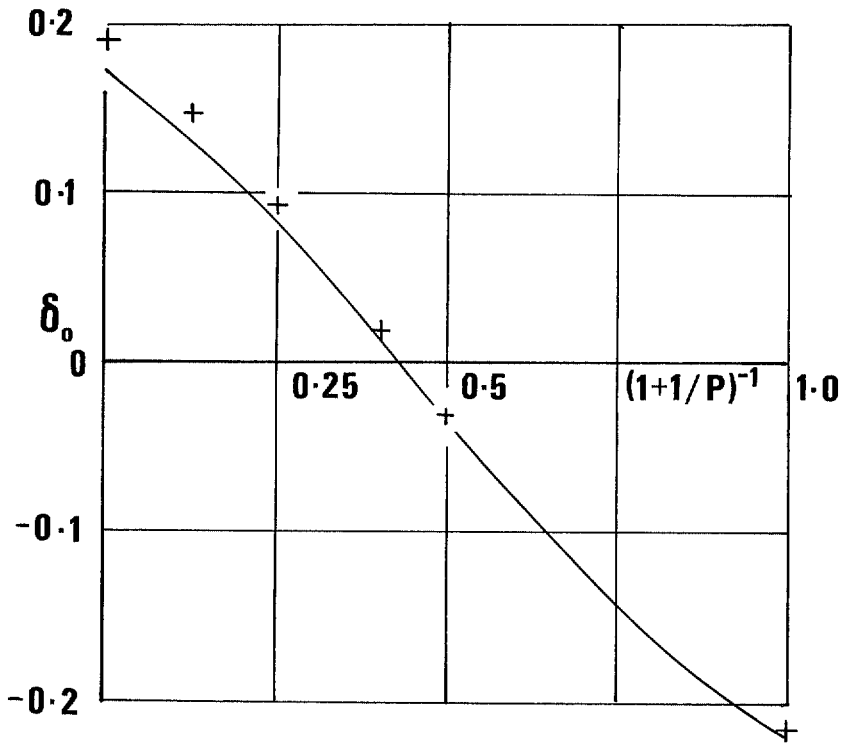


FIG. 2. Finite difference mesh showing fictitious node (1).



———— Theoretical result from Ref. 5      + Present method,  $wh/U=0.01$

FIG. 3. Variation of  $\delta_0$  in rectangular tunnels with non-ideal slotted roof and floor ( $F=0.233$ ).

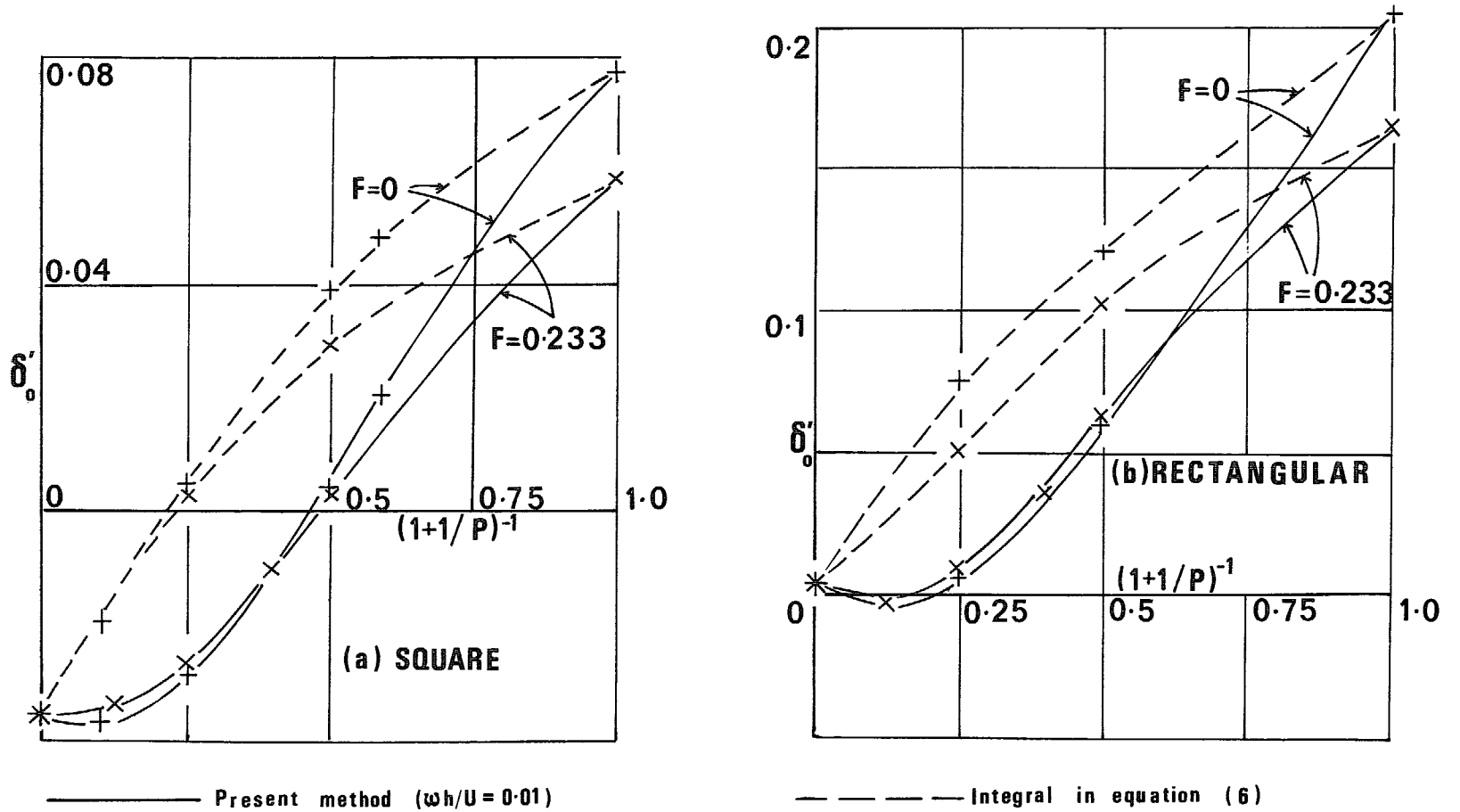
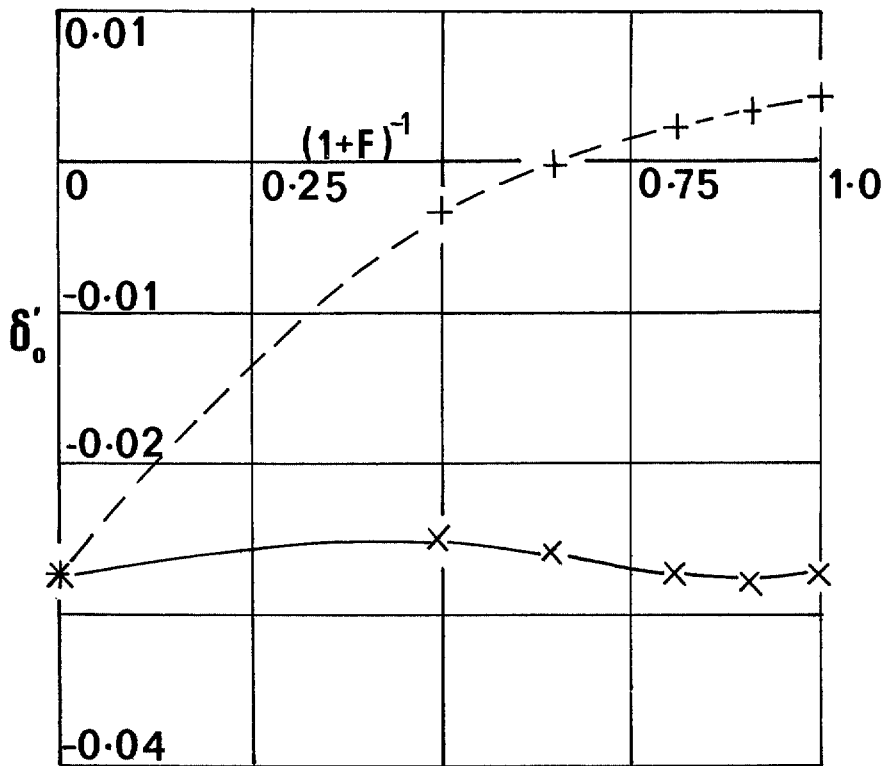


FIG. 4. Comparison of two definitions of  $\delta_0$  for tunnels with perforated or porous-slotted roof and floor.



—x— Present method ( $\omega h/U = 0.01$ ). —+— Integral equation (6).

FIG. 5. Comparison of two definitions of  $\delta_0'$  for square tunnels with slotted roof and floor of fixed porosity ( $1/P = 3.0$ ).

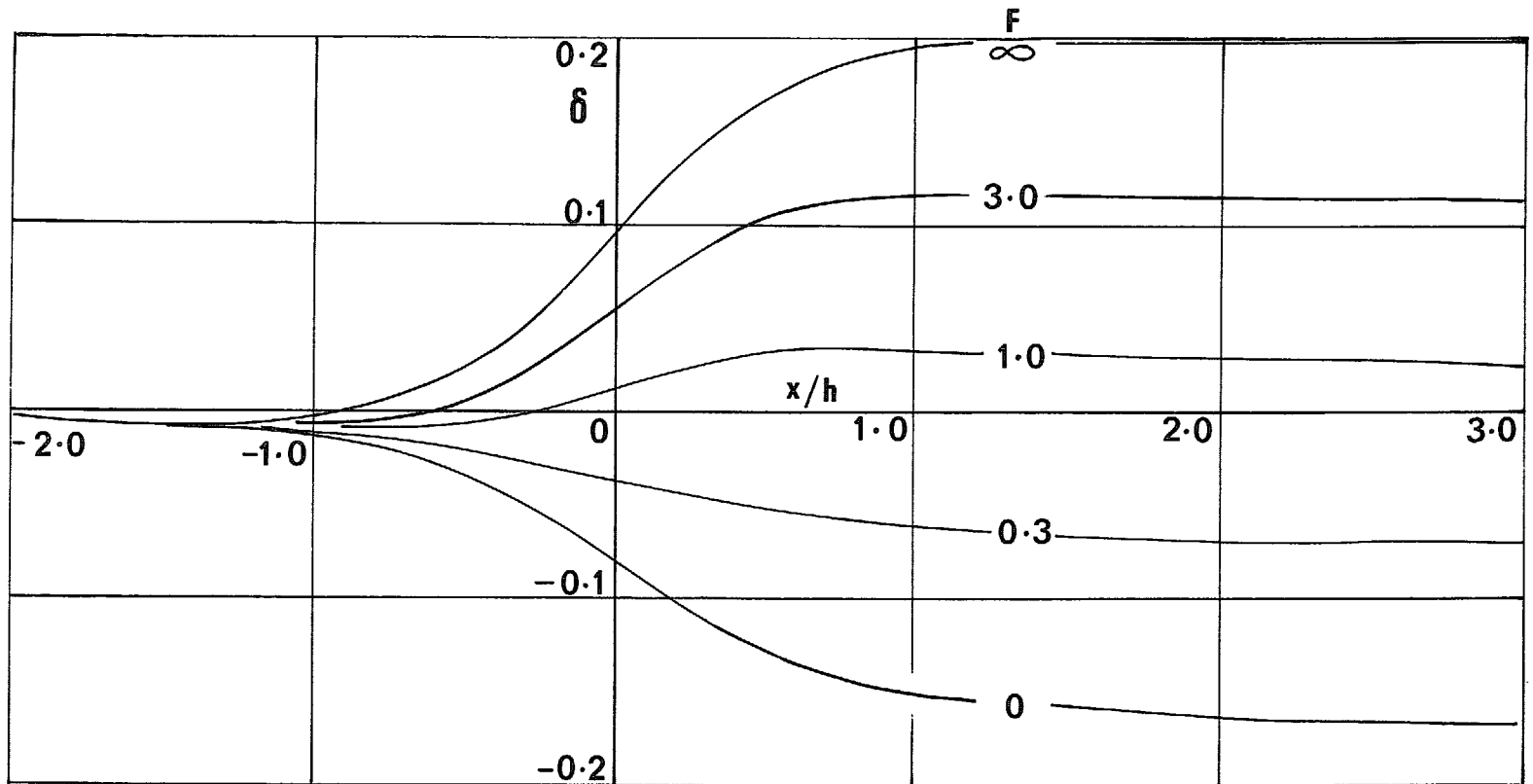


FIG. 6. Streamwise distribution of  $\delta$  for square tunnels with ideal-slotted roof and floor.

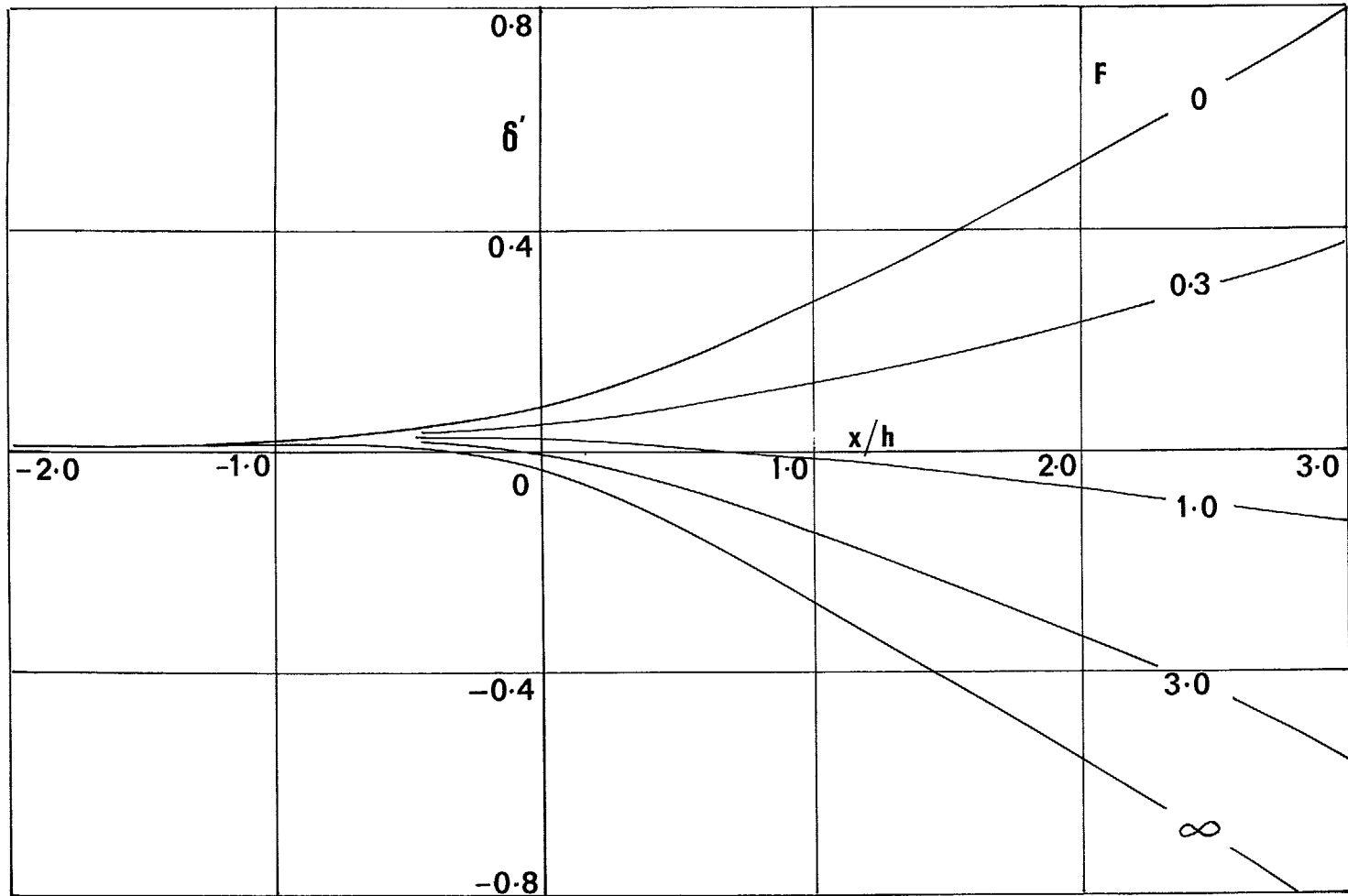


FIG. 7. Streamwise distribution of  $\delta'$  for square tunnels with ideal-slotted roof and floor.

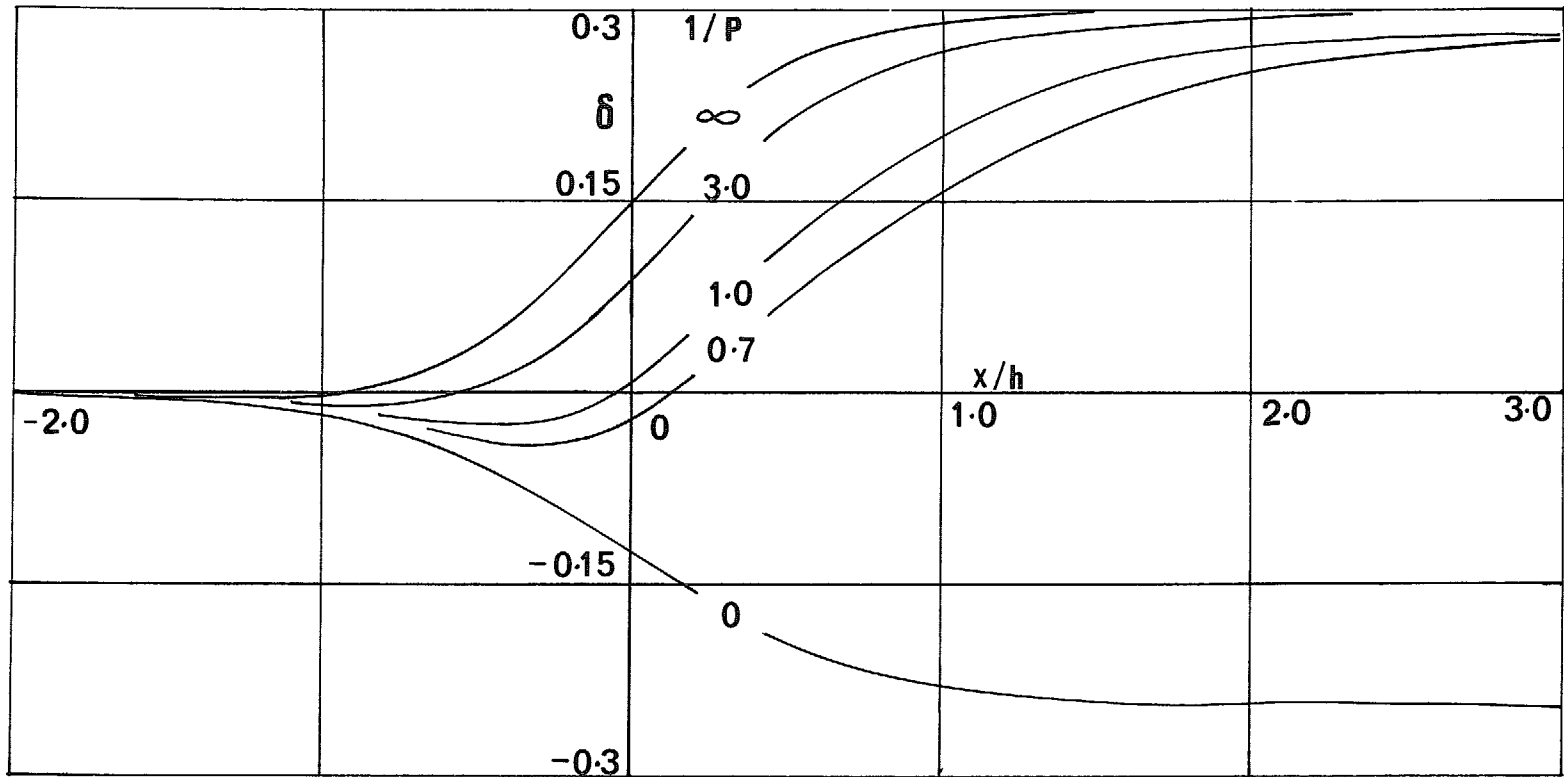


FIG. 8. Streamwise distribution of  $\delta$  for square tunnels with perforated roof and floor.

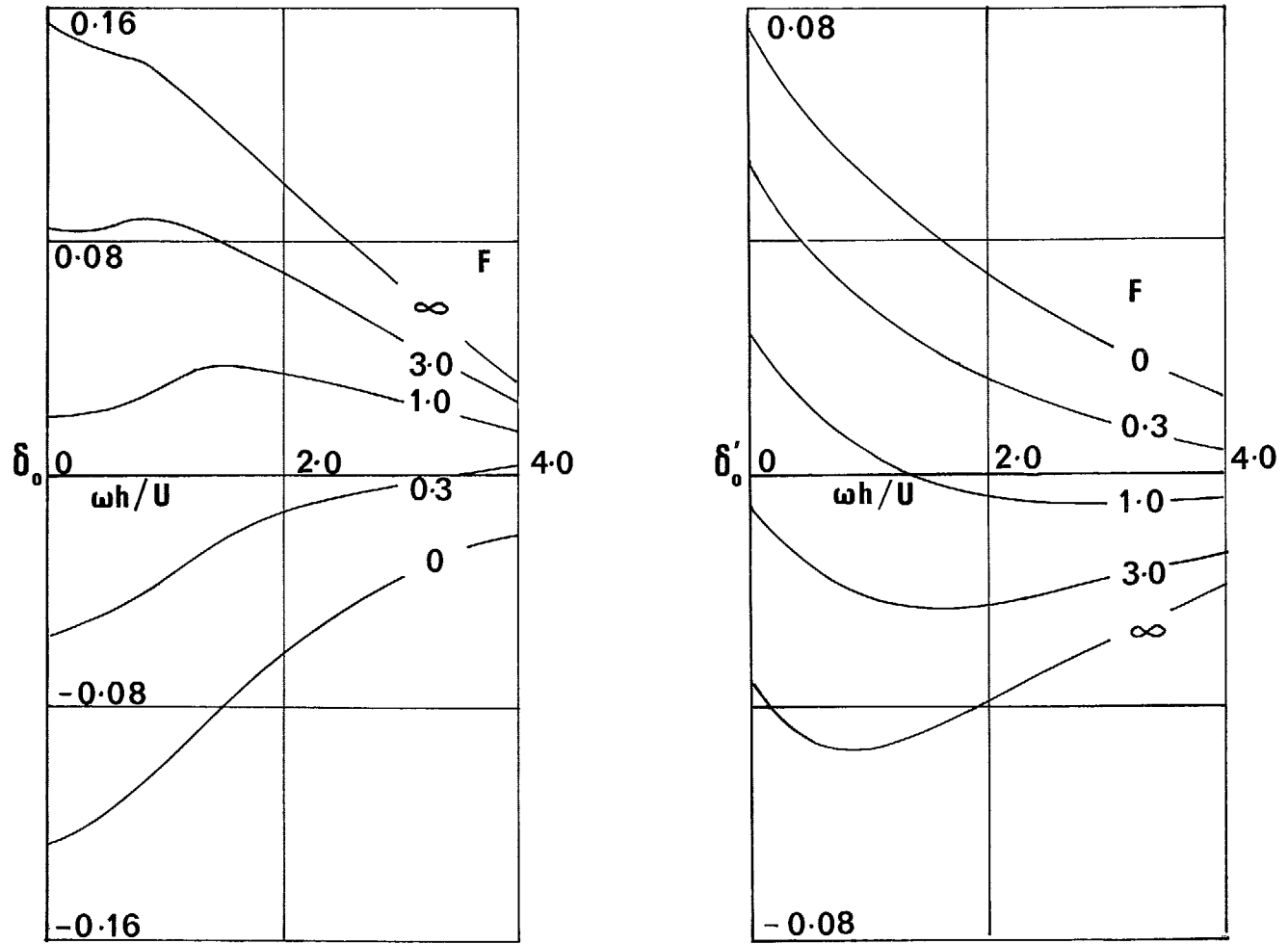


FIG. 9. Frequency effect for square tunnels with ideal-slotted roof and floor.

# Part II—Oscillatory Lift Interference in Subsonic Compressible Flow

## *Summary*

This report describes a method of calculating the oscillatory lift-interference parameters in subsonic compressible flow for ventilated wind tunnels. Results are obtained by solving the finite-difference form of the governing equations using the dynamic-relaxation method.

Detailed results are obtained at  $M=0.7$  for square tunnels with closed side walls and with a variety of conditions on the roof and floor. As the frequency of the oscillations is increased different trends are noted between the present compressible flow parameters and earlier incompressible results.

## LIST OF CONTENTS

1. Introduction
2. Mathematical Formulation
  - 2.1. Governing Equations
  - 2.2. Boundary Conditions
  - 2.3. Small Wing
  - 2.4. Interference Upwash
  - 2.5. Non-dimensional Form
  - 2.6. Interference Upwash Parameters
3. Numerical Solution
  - 3.1. Differential Equation
  - 3.2. Boundary Conditions
  - 3.3. Infinite Integral for Small Wing
  - 3.4. Solution for Interference Potential
  - 3.5. Solution on Digital Computer
4. Comparison with Low-Frequency Results
5. Investigation of a Square Tunnel
  - 5.1. Details of Solutions
  - 5.2. Discussion of Results

Acknowledgement

List of Symbols

References

Tables 1 and 2

Illustrations—Figs. 1 to 6

Detachable Abstract Cards

## 1. Introduction

In a series of papers, theoretical solutions have been obtained for the lift interference in ventilated wind tunnels. Initially the velocity potential in the distant wake of an oscillating wing was considered; this required the solution of a Poisson equation in two dimensions<sup>1</sup>. Next the three-dimensional problem of the steady lift interference in both slotted and perforated tunnels was examined<sup>2</sup>. In Part I of this Report this treatment was extended to include oscillatory incompressible flow, and Part II develops the technique further to include compressible oscillatory flow.

The solutions are obtained by writing the governing differential equations with the associated boundary conditions in finite-difference form and the resulting equations are solved by using either a resistance-network analogue or a digital computer. When many results are required it is convenient to use the digital method; much of the development work, however, was carried out on the resistance analogue. Several digital-computer methods are available for solving finite-difference equations, but when complicated boundary conditions apply, the dynamic-relaxation technique has proved to be most suitable.

Since the object of these studies is to determine interference parameters, a solution is obtained initially in terms of the perturbation velocity potential; this is followed by a second solution in terms of the interference velocity potential. The boundary values of the interference potential are calculated from the difference between the perturbation velocity potentials of the model in constrained and unconstrained flow. Each of these three velocity potentials satisfies the same differential equation.

The report first shows how the previous work is extended to include compressible flow, and the validity of the method is checked by correlating the low-frequency results in compressible and incompressible flow. Then a description is given of detailed investigations into the effect of frequency on the interference parameters for square tunnels, with a range of different conditions on the roof and floor.

## 2. Mathematical Formulation

As in previous studies of lift interference in rectangular ventilated tunnels, the formulation of the problem involves the specification of the governing equation, boundary condition and disturbance due to a wing positioned at the centre of the tunnel. Once a solution to the problem has been obtained, the results are expressed as interference upwash parameters. The relevant equations for compressible oscillatory flow are given below. The coordinate system is illustrated in Fig. 1.

### 2.1 Governing Equations

The linearized equation for the complex velocity potential,  $\bar{\phi}$ , in subsonic compressible flow is:

$$\beta^2 \frac{\partial^2 \bar{\phi}}{\partial x^2} + \frac{\partial^2 \bar{\phi}}{\partial y^2} + \frac{\partial^2 \bar{\phi}}{\partial z^2} - \frac{2i\omega M^2}{U} \frac{\partial \bar{\phi}}{\partial x} + \frac{\omega^2 M^2 \bar{\phi}}{U^2} = 0.$$

This equation can be simplified in terms of the modified potential

$$\bar{\psi} = \bar{\phi} \exp\left(-\frac{i\omega M^2 x}{\beta^2 U}\right), \quad (1)$$

giving

$$\beta^2 \frac{\partial^2 \bar{\psi}}{\partial x^2} + \frac{\partial^2 \bar{\psi}}{\partial y^2} + \frac{\partial^2 \bar{\psi}}{\partial z^2} + \frac{\omega^2 M^2 \bar{\psi}}{\beta^2 U^2} = 0. \quad (2)$$

Each of the three velocity potentials,  $\bar{\psi}$ ,  $\bar{\psi}_m$  and  $\bar{\psi}_i$ , must satisfy this differential equation.

## 2.2 Boundary Conditions

The general boundary condition at a porous slotted wall from equation (6) of Ref. 4

$$\left(\frac{\partial}{\partial x} + \frac{i\omega}{U}\right)\left(\bar{\phi} + K \frac{\partial \bar{\phi}}{\partial n}\right) + \frac{1}{P} \frac{\partial \bar{\phi}}{\partial n} = 0,$$

when expressed in terms of the modified potential

$$\bar{\psi} = \psi_R + i\psi_I,$$

gives two real conditions

$$\text{and } \left. \begin{aligned} \frac{\partial \psi_R}{\partial x} - \frac{\omega \psi_I}{\beta^2 U} + K \left( \frac{\partial^2 \psi_R}{\partial x \partial n} - \frac{\omega}{\beta^2 U} \frac{\partial \psi_I}{\partial n} \right) + \frac{1}{P} \frac{\partial \psi_R}{\partial n} = 0 \\ \frac{\partial \psi_I}{\partial x} + \frac{\omega \psi_R}{\beta^2 U} + K \left( \frac{\partial^2 \psi_I}{\partial x \partial n} + \frac{\omega}{\beta^2 U} \frac{\partial \psi_R}{\partial n} \right) + \frac{1}{P} \frac{\partial \psi_I}{\partial n} = 0 \end{aligned} \right\} \quad (3)$$

For closed and open walls these become

$$\frac{\partial \psi_R}{\partial n} = \frac{\partial \psi_I}{\partial n} = 0$$

and

$$\psi_R = \psi_I = 0 \text{ respectively.}$$

## 2.3 Small Wing

In this report the lift interference under consideration is that due to a small wing. The simplest expression for the undisturbed velocity potential due to a small wing with oscillatory lift at arbitrary subsonic Mach number is

$$\bar{\phi}_m = -\frac{US\bar{C}_L}{8\pi} \frac{\partial}{\partial z} \left[ \int_0^\infty \frac{1}{r} \exp\left(-\frac{i\omega}{\beta^2 U}(x' - M^2 x + Mr)\right) dx' \right],$$

where

$$r^2 = (x - x')^2 + \beta^2(y^2 + z^2).$$

Substitution of equation (1) into the above equation gives

$$\bar{\psi}_m = \frac{US\bar{C}_L \beta^2 z}{8\pi} \int_0^\infty \left(1 + \frac{i\omega Mr}{\beta^2 U}\right) \exp\left(-\frac{i\omega}{\beta^2 U}(x' + Mr)\right) \frac{dx'}{r^3}. \quad (4)$$

## 2.4 Interference Upwash

Finally the interference upwash is expressed in terms of the modified interference potential, so that

$$\bar{w}_i = \frac{\partial \bar{\phi}_i}{\partial z} = \exp\left(\frac{i\omega M^2 x}{\beta^2 U}\right) \frac{\partial \bar{\psi}_i}{\partial z}. \quad (5)$$

## 2.5 Non-dimensional Form

Equations (2) to (5) can be written in non-dimensional form after the following substitutions:

$$x = \frac{1}{2}\beta h X, \quad y = \frac{1}{2}h Y, \quad z = \frac{1}{2}k Z, \quad n = \frac{1}{2}h N, \quad K = \frac{1}{2}h F, \quad \bar{\psi} = (US\bar{C}_L/2b)\bar{\Psi}, \quad \omega = 2Uv/h \quad \text{and} \quad \bar{w}_i = (US\bar{C}_L/bh)\delta.$$

The non-dimensional equations are;

$$\frac{\partial^2 \bar{\Psi}}{\partial X^2} + \frac{\partial^2 \bar{\Psi}}{\partial Y^2} + \frac{\partial^2 \bar{\Psi}}{\partial Z^2} + \frac{v^2 M^2 \bar{\Psi}}{\beta^2} = 0, \quad (2a)$$

$$\left. \begin{aligned} \frac{\partial \bar{\Psi}_R}{\partial X} - \frac{v \bar{\Psi}_I}{\beta} + F \left( \frac{\partial^2 \bar{\Psi}_R}{\partial X \partial N} - \frac{v}{\beta} \frac{\partial \bar{\Psi}_I}{\partial N} \right) + \frac{\beta}{P} \frac{\partial \bar{\Psi}_R}{\partial N} = 0 \\ \frac{\partial \bar{\Psi}_I}{\partial X} + \frac{v \bar{\Psi}_R}{\beta} + F \left( \frac{\partial^2 \bar{\Psi}_I}{\partial X \partial N} + \frac{v}{\beta} \frac{\partial \bar{\Psi}_R}{\partial N} \right) + \frac{\beta}{P} \frac{\partial \bar{\Psi}_I}{\partial N} = 0 \end{aligned} \right\}, \quad (3a)$$

$$\bar{\Psi}_m = \frac{bZ}{2\pi h} \int_0^\infty \left( 1 + \frac{ivMR}{\beta} \right) \exp \left( \frac{-iv}{\beta} (X' + MR) \right) \frac{dX'}{R^3} \quad (4a)$$

where

$$R = [(X - X')^2 + Y^2 + Z^2]^{\frac{1}{2}} \quad \text{and}$$

$$\delta = \exp \left( \frac{ivM^2 X}{\beta} \right) \frac{\partial \bar{\Psi}_i}{\partial Z}. \quad (5a)$$

## 2.6 Interference Upwash Parameters

The interference upwash parameter,  $\delta$ , in compressible flow is defined as

$$\delta = \left[ \left\{ \delta_0(M) + \delta_1(M) \frac{x}{h} + \delta_2(M) \left( \frac{x}{h} \right)^2 + \dots \right\} + \frac{i\omega h}{U} \left\{ \delta_0'(M) + \delta_1'(M) \frac{x}{h} + \delta_2'(M) \left( \frac{x}{h} \right)^2 + \dots \right\} \right]. \quad (6)$$

Hence

$$\left. \begin{aligned} \delta_0(M) &= (\delta_R)_{x=0}, & \delta_0'(M) &= \frac{U}{\omega h} (\delta_I)_{x=0} \\ \delta_1(M) &= h \left( \frac{\partial \delta_R}{\partial x} \right)_{x=0}, & \delta_1'(M) &= \frac{U}{\omega} \left( \frac{\partial \delta_I}{\partial x} \right)_{x=0} \\ \delta_2(M) &= \frac{h^2}{2} \left( \frac{\partial^2 \delta_R}{\partial x^2} \right)_{x=0}, & \delta_2'(M) &= \frac{hU}{2\omega} \left( \frac{\partial^2 \delta_I}{\partial x^2} \right)_{x=0} \end{aligned} \right\}. \quad (7)$$

The six interference parameters can therefore be determined from the real and imaginary parts of  $\delta$  given by equation (5a), namely

$$\left. \begin{aligned} \delta_R &= \frac{\partial \Psi_{iR}}{\partial Z} \cos\left(\frac{vM^2 X}{\beta}\right) - \frac{\partial \Psi_{iI}}{\partial Z} \sin\left(\frac{vM^2 X}{\beta}\right) \\ \delta_I &= \frac{\partial \Psi_{iR}}{\partial Z} \sin\left(\frac{vM^2 X}{\beta}\right) + \frac{\partial \Psi_{iI}}{\partial Z} \cos\left(\frac{vM^2 X}{\beta}\right) \end{aligned} \right\} \quad (5b)$$

and

### 3. Numerical Solution

#### 3.1 Differential Equation

The differential equation for compressible flow

$$\frac{\partial^2 \bar{\Psi}}{\partial X^2} + \frac{\partial^2 \bar{\Psi}}{\partial Y^2} + \frac{\partial^2 \bar{\Psi}}{\partial Z^2} + \frac{v^2 M^2 \bar{\Psi}}{\beta^2} = 0, \quad (2a)$$

can be solved by a dynamic-relaxation method similar to that for incompressible flow described in Ref. 3. For incompressible flow the Laplace equation in three dimensions applies, but with compressible flow there is the additional term  $v^2 M^2 \bar{\Psi} / \beta^2$ .

A solution to this complex equation can be obtained by dividing it into real and imaginary parts

$$\frac{\partial^2 \Psi_R}{\partial X^2} + \frac{\partial^2 \Psi_R}{\partial Y^2} + \frac{\partial^2 \Psi_R}{\partial Z^2} + \frac{v^2 M^2 \Psi_R}{\beta^2} = 0 \quad (2b)$$

and

$$\frac{\partial^2 \Psi_I}{\partial X^2} + \frac{\partial^2 \Psi_I}{\partial Y^2} + \frac{\partial^2 \Psi_I}{\partial Z^2} + \frac{v^2 M^2 \Psi_I}{\beta^2} = 0. \quad (2c)$$

Each equation can be written in finite-difference form and solved separately, but simultaneously. For each part, auxiliary variables  $u$ ,  $v$  and  $w$  are introduced in the three following equations:

$$\left. \begin{aligned} \frac{\partial u}{\partial t} + Du &= \frac{\partial \Psi_R}{\partial X}, \\ \frac{\partial v}{\partial t} + Dv &= \frac{\partial \Psi_R}{\partial Y}, \\ \text{and } \frac{\partial w}{\partial t} + Dw &= \frac{\partial \Psi_R}{\partial Z}, \end{aligned} \right\} \quad (8)$$

which when substituted into

$$\frac{\partial u}{\partial X} + \frac{\partial v}{\partial Y} + \frac{\partial w}{\partial Z} + \frac{v^2 M^2 \Psi_R}{D\beta^2} = \frac{\partial \Psi_R}{\partial t} \quad (9)$$

leads to equation (2b), with an acceleration and a velocity term added.

Using the same type of graded net as in Fig. 1 of Ref. 3, the equations can be written in an explicit finite-difference form and solved by a substitution routine on a digital computer.

### 3.2 Boundary Conditions

The boundary conditions in equation (3a) are included in the finite-difference solution through fictitious nodes positioned at one mesh interval outside the boundaries. Values at these fictitious nodes can be calculated if the normal slope of the function is known. Thus the first condition is written with the normal slope on the left hand side;

$$\frac{\partial \Psi_R}{\partial N} = \left(\frac{\beta}{P}\right)^{-1} \left[ -\frac{\partial \Psi_R}{\partial X} + \frac{v \Psi_I}{\beta} - F \left( \frac{\partial^2 \Psi_R}{\partial X \partial N} - \frac{v \partial \Psi_I}{\beta \partial N} \right) \right]. \quad (10)$$

The finite-difference form of this equation is similar to equation (16) of Part I of this report. The right hand side of this equation specifies the value of the normal slope and depends on both the real and imaginary parts of the velocity potential. It is for this reason that the equations for the real and imaginary parts must be solved simultaneously.

If a boundary is closed,  $\beta/P$  equals infinity and equation (10) simplifies to  $\partial \Psi_R / \partial N = 0$ . Alternatively, if a boundary is open, then the boundary conditions as stated in Section 2.2 are enforced directly as  $\Psi_R = 0$  and  $\Psi_I = 0$  on the boundary.

### 3.3 Infinite Integral for Small Wing

One method of calculating the infinite integral for the velocity potential due to a small wing in incompressible flow was described in Section 4.1 of Part I. This method involves a separate evaluation of the infinite integral by the trapezoidal rule with small step lengths for each node around the wing and on the roof and walls. Since this takes considerable time on the digital computer, equation (4a) was rearranged as follows:

$$\bar{\Psi}_m = \frac{bZ}{2\pi h} \exp\left(-\frac{ivX}{\beta}\right) \int_{-x}^{\infty} \left(1 + \frac{ivMR_0}{\beta}\right) \exp\left(\frac{-iv}{\beta}(X_0 + MR_0)\right) \frac{dX_0}{R_0^3} \quad (11)$$

where  $R_0^2 = X_0^2 + Y^2 + Z^2$ .

The advantage of writing the equation in this form is apparent by considering the evaluation of  $\bar{\Psi}_m$  on a line of nodes with constant  $Y$  and  $Z$  but with variable  $X$ . If the plane furthest upstream is taken as a datum and denoted by  $\bar{X}$ , the value of  $\Psi_m$  at all other planes with the same  $Y$  and  $Z$  can be calculated from

$$\begin{aligned} \bar{\Psi}_m = \frac{bZ}{2\pi h} \exp\left(\frac{-ivX}{\beta}\right) & \left[ \int_{-\bar{X}}^{\infty} \left(1 + \frac{ivMR_0}{\beta}\right) \exp\left(\frac{-iv}{\beta}(X_0 + MR_0)\right) \frac{dX_0}{R_0^3} + \right. \\ & \left. + \int_{-x}^{-\bar{X}} \left(1 + \frac{ivMR_0}{\beta}\right) \exp\left(\frac{-iv}{\beta}(X_0 + MR_0)\right) \frac{dX_0}{R_0^3} \right]. \quad (12) \end{aligned}$$

Thus the value of  $\bar{\Psi}_m$  at each value of  $X$  can be calculated from a single infinite integral plus an integral between finite limits. This leads to a considerable saving in computer time.

### 3.4 Solution for Interference Potential

After obtaining a solution in terms of the velocity potential  $\bar{\Psi}$ , a second solution is required in terms of the interference potential  $\bar{\Psi}_i$ . Since  $\bar{\Psi}_i$  also satisfies the governing equation (2a), the same finite-difference

programme can be used. The boundary conditions are that in the plane of the wing  $Z=0$ ,  $\Psi_{iR} = \Psi_{iI} = 0$ , on the plane  $Y=0$  symmetry occurs with  $\partial\Psi_{iR}/\partial Y = 0$ ,  $\partial\Psi_{iI}/\partial Y = 0$ , whilst on the roof and walls

$$\left. \begin{aligned} \Psi_{iR} &= \Psi_R - \Psi_{mR} \\ \Psi_{iI} &= \Psi_I - \Psi_{mI} \end{aligned} \right\} \quad (13)$$

The interference upwash is calculated from the interference potentials using equations (5b). By fitting a third-order polynomial the terms  $\partial\Psi_{iR}/\partial Z$  and  $\partial\Psi_{iI}/\partial Z$  can be calculated from values on the finite-difference mesh. Section 4.6 of Part I contains further details and also explains the method of determining the derivatives  $\partial\delta/\partial x$  and  $\partial^2\delta/\partial x^2$  that are required to calculate interference parameters from equations (7).

### 3.5 Solution on Digital Computer

If a sufficiently fine mesh is used, then the finite-difference solution approaches the true solution to the differential equation. However, there is a practical restriction on the number of mesh intervals that can be used. This is primarily due to the limited size of the fast store of digital computers. With the KDF 9 used in the present investigation the total size of the fast store is 32K, restricting the number of nodal points to 24, 9 and 9 in the  $X$ ,  $Y$  and  $Z$  directions respectively, which include the fictitious nodes surrounding the boundaries. Since the equations for both the real and imaginary parts have to be solved simultaneously, this mesh spacing is equivalent to about 4000 unknowns in the dynamic-relaxation calculation. This restriction on the number of nodes does lead to some errors which can only be overcome by means of a larger computer.

Since dynamic relaxation is an iterative method, efficient solutions can only be obtained with optimum values of the damping factor  $D$  in equations (8) and (9) and time interval  $\Delta t$  of Ref. 3. For the open, closed and slotted boundaries, the convergence parameters are similar to those listed for a closed tunnel in Section 4.5 of Part I, but for the porous slotted boundaries several trial values are required before suitable convergence parameters are obtained. It is important to calculate the residuals in order to check that each result is an adequate solution to the finite-difference equations.

## 4. Comparison with Low-Frequency Results

The reliability of this present method of analysing compressible flow can be investigated by making a comparison with results obtained from an alternative approach. Such a comparison is possible for low frequency.

For low-frequency compressible flow, the interference upwash can be deduced from equation (12) of Ref. 4 to be

$$\delta = \left[ 1 + \frac{i\omega M^2 x}{\beta^2 U} \right] \left[ \left( \delta_0(0) + \delta_1(0) \frac{x}{\beta h} + \delta_2(0) \left( \frac{x}{\beta h} \right)^2 + \dots \right) + \frac{i\omega h}{\beta U} \left( \delta_0'(0) + \delta_1'(0) \frac{x}{\beta h} + \delta_2'(0) \left( \frac{x}{\beta h} \right)^2 + \dots \right) \right] \quad (14)$$

where  $\delta_0(0)$ ,  $\delta_1(0)$  etc. are the interference parameters at low frequency and zero Mach number. Values of these parameters have already been obtained from analytical and finite-difference solutions and are reported in Part I.

The compressible equations can also be used to obtain values of the interference parameters for low frequency. A value of  $\omega h/U = 0.01$  is used, as this has been found to give effectively the same result as in

the limit  $\omega \rightarrow 0$ . When equations (14) and (6) are identified, the following relationships are obtained.

$$\left. \begin{aligned} \delta_0(M) &= \delta_0(0), \\ \delta_1(M) &= \beta^{-1} \delta_1(0), \\ \delta_2(M) &= \beta^{-2} \delta_2(0), \\ \delta_0'(M) &= \beta^{-1} \delta_0'(0), \\ \delta_1'(M) &= \beta^{-2} [\delta_1'(0) + M^2 \delta_0(0)] \\ \text{and } \delta_2'(M) &= \beta^{-3} [\delta_2'(0) + M^2 \delta_1(0)] \end{aligned} \right\} \quad (15)$$

Comparisons are made for  $M = 0.7$  for a square tunnel with five different boundary conditions on the roof and floor, and the results are recorded in Table 1. The results in columns A are taken from Table 2 of Part I, whilst the compressible flow solutions in columns B are obtained by the method described in Section 3. The agreement is good for all but  $\delta_2$  and  $\delta_2'$ . Such inaccuracies can be anticipated since  $\delta_2$  and  $\delta_2'$  are calculated from a third differential of the interference upwash.

## 5. Investigation of a Square Tunnel

### 5.1 Details of Solutions

A systematic investigation has been carried out for a square tunnel having closed side walls and with five different conditions on the roof and floor. These are,

- Case 1. Closed roof and floor  $(1 + F)^{-1} = \text{any}$ ,  $(1 + \beta/P)^{-1} = 0$ ; alternatively this can be written as  $(1 + F)^{-1} = 0.811$ ,  $(1 + \beta/P)^{-1} = 0$ .
- Case 2. Porous slotted roof and floor  $(1 + F)^{-1} = 0.811$ ,  $(1 + \beta/P)^{-1} = 0.25$ .
- Case 3. Porous slotted roof and floor  $(1 + F)^{-1} = 0.811$ ,  $(1 + \beta/P)^{-1} = 0.5$ .
- Case 4. Ideal slotted roof and floor  $(1 + F)^{-1} = 0.811$ ,  $(1 + \beta/P)^{-1} = 1.0$ .
- Case 5. Open roof and floor  $(1 + F)^{-1} = 1.0$ ,  $(1 + \beta/P)^{-1} = 1.0$ .

One particular value of the Mach number is taken,  $M = 0.7$ , with the frequency parameter varying from 0.01 to 3.0.

The solutions were obtained on a graded finite-difference mesh having between 19 and 22 mesh nodes representing the length of the tunnel and seven mesh nodes representing the half height and half breadth of the tunnel. The smallest mesh interval of 0.05 of the height of the tunnel is at the origin of the tunnel where the model is situated.

The dynamic-relaxation procedure required at least 300 iterations in calculating values of  $\Psi_R$  and  $\Psi_I$  throughout the field, and 250 iterations for  $\Psi_{iR}$  and  $\Psi_{iI}$ . However, with the closed and the porous slotted tunnels slightly more iterations were necessary. An increase in iterations was also required as the frequency increased, probably due to the more rapid changes in the magnitude of the functions occurring at higher frequencies. It was not possible to obtain any converged results for values of the porosity parameter  $0.5 < (1 + \beta/P)^{-1} < 1$ ; similar difficulties were encountered with steady incompressible flow<sup>2</sup>.

Table 2 lists the interference parameters for each of the five cases. Because a finite-difference approximation is used certain errors will occur but, following Part I, it is estimated that no result is in error by more than 0.01. Note that these are not random errors due to an inaccurate numerical solution, but they are consistent errors arising from the finite-difference approximation to the differential equation. These errors are largest with the closed boundaries and become less as the boundary tends to the open condition.

## 5.2 Discussion of Results

The consistency of the results is checked by plotting each of the interference parameters against frequency. Graphs of  $\delta_0$ ,  $\delta_0'$ ,  $\delta_1$ ,  $\delta_1'$  for each of the five cases are included as Fig. 2 and 3.

One important fact is that  $\delta_0$ , and  $\delta_0'$  tend to high values as  $\omega h/U$  increases. This is in marked contrast to the incompressible case where both  $\delta_0$  and  $\delta_0'$  tend to zero as the frequency increases. This difference is illustrated in Fig. 4 where certain results for compressible flow (full curves numbered 1C, 4C, 5C) are compared with incompressible results for the same boundary conditions taken from Part I (broken curves numbered 1I, 4I, 5I).

Tunnel resonance is the probable cause of the increasing values of interference parameters with increasing frequency. From Ref. 5 calculations can be made of the resonant frequency; for a three-dimensional tunnel with closed boundaries and  $M=0.7$  the resonance occurs when  $\omega h/U=3.205$ . As this frequency is approached, the interference parameters become large. A dynamic-relaxation result has been obtained for a closed tunnel with  $\omega h/U=3.0$ . The parameters  $\delta_0=0.33$  and  $\delta_0'=-0.46$  are large, indicating that tunnel resonance is being approached. These results are not included in Table 2 since they are not of the same accuracy as other results. For the fully open tunnel the critical frequency is  $\omega h/U=6.41$ , and therefore with cases 4 and 5, which tend towards the fully open condition, there is no difficulty in obtaining dynamic-relaxation results for  $\omega h/U=3.0$ .

A further comparison is given in Fig. 5 by plotting the variation of  $\delta_0$  and  $\delta_0'$  at  $M=0.7$  for porous slotted tunnels against the porosity parameter  $(1+\beta/P)^{-1}$  with the slot parameter  $(1+F)^{-1}$  remaining constant at 0.811. Although results have not been obtained in the range  $0.5 < (1+\beta/P)^{-1} < 1.0$ , it seems reasonable to anticipate smooth curves through this region. Fig. 5 also contains results for incompressible flow at vanishing frequency. For  $\delta_0$  the incompressible curve lies directly on top of the compressible result with  $\omega h/U=0$ , but for  $\delta_0'$  the compressible and incompressible curves differ by the factor  $\beta$  in accord with equations (15). These curves indicate that, as the frequency increases to a value of  $\omega h/U=2.0$  or greater, then the interference parameters are significantly different from those for low frequency.

Finally Fig. 6 shows the variation of the interference parameters,  $\delta_1$  and  $\delta_1'$ , with Mach number for a square porous slotted tunnel with  $(1+F)^{-1}=0.811$  and  $(1+\beta/P)^{-1}=0.5$ . From the relationships of Section 4 it is possible to calculate the values of the parameters at zero frequency for any Mach number. These results are shown as smooth curves. Fig. 6 also includes values of  $\delta_1$  and  $\delta_1'$  for non-zero frequencies when  $M=0$  and 0.7.

### Acknowledgement

The authors wish to acknowledge the help given by Mr. H. C. Garner of the National Physical Laboratory with the theoretical aspects of this study.

## LIST OF SYMBOLS

|   |   |
|---|---|
| $b$   | Tunnel breadth  |
| $\bar{C}_L$   | Complex lift coefficient  |
| $D$   | Damping factor  |
| $F$   | Non-dimensional slot parameter = $2K/h$   |
| $h$   | Tunnel height   |
| $K$   | Geometric slot parameter  |
| $M$   | Mach number   |
| $n$   | Outward normal distance from boundary   |
| $N$   | Non-dimensional distance from boundary = $2n/h$   |
| $P$   | Porosity parameter  |
| $S$   | Planform area of wing   |
| $t$   | Non-dimensional time  |
| $U$   | Velocity of undisturbed stream  |
| $u, v, w$   | Auxiliary variables in equation (8)   |
| $\bar{w}_i$   | Complex interference upwash   |
| $x, y, z$   | Cartesian coordinates (Fig. 1)  |
| $X, Y, Z$   | Non-dimensional coordinates $2x/\beta h, 2y/h, 2z/h$  |
| $x', X'$  | Increment in streamwise direction   |
| $\beta$   | $(1 - M^2)^{\frac{1}{2}}$   |
| $\delta$  | Distribution of interference upwash along the tunnel = $\frac{bh\bar{w}_i}{US\bar{C}_L}$                      |
| $\delta_0, \delta_1, \delta_2$<br>$\delta_0', \delta_1', \delta_2'$ | Interference parameters defined in equation (6)   |
| $v$   | Non-dimensional frequency of oscillation = $\frac{1}{2}\omega h/U$  |
| $\bar{\psi}$  | Complex modified potential, $\bar{\psi} = \bar{\phi} \exp\left(-\frac{i\omega M^2 x}{\beta^2 U}\right)$       |
| $\bar{\Psi}$  | Complex non-dimensional modified potential $\bar{\Psi} = \frac{2b\bar{\psi}}{US\bar{C}_L} = \Psi_R + i\Psi_I$ |

LIST OF SYMBOLS—*continued*

|                |   |
|----------------|---|
| $\bar{\Psi}_m$ | $\bar{\Psi}$ in unconstrained flow, $\bar{\Psi}_m = \Psi_{mR} + i \Psi_{mI}$                |
| $\bar{\Psi}_i$ | Modified interference potential, $\bar{\Psi}_i = \Psi_{iR} + i \Psi_{iI}$                   |
| $\bar{\phi}$   | Complex perturbation velocity potential $\bar{\phi} = \phi_R + i \phi_I$                    |
| $\bar{\phi}_m$ | Velocity potential of model in unconstrained flow, $\bar{\phi}_m = \phi_{mR} + i \phi_{mI}$ |
| $\bar{\phi}_i$ | Interference potential, $\bar{\phi}_i = \phi_{iR} + i \phi_{iI}$                            |
| $\omega$       | Angular frequency of oscillation  |

## REFERENCES

| <i>No.</i> | <i>Author(s)</i>   | <i>Title, etc.</i>  |
|------------|--|---|
| 1          | K. R. Rushton . . . . .                                      | Studies of slotted-wall interference using an electrical analogue.<br>A.R.C. R. & M. 3452 (1965).   |
| 2          | K. R. Rushton and<br>Lucy M. Laing . . . . .                 | A general method of studying steady lift interference in slotted<br>and perforated tunnels.<br>A.R.C. R. & M. 3567 (1967).  |
| 3          | K. R. Rushton and<br>Lucy M. Laing . . . . .                 | A digital computer solution of the Laplace equation using the<br>Dynamic Relaxation method.<br>Aeron. Quart., Vol. XIX, Pt. 4, Nov. 1968, pp. 375–387.                          |
| 4          | H. C. Garner, A. W. Moore . . .<br>and K. C. Wight . . . . . | The theory of interference effects on dynamic measurements in<br>slotted-wall tunnels at subsonic speeds and comparisons with<br>experiment.<br>A.R.C. R. & M. No. 3500 (1966). |
| 5          | W. E. A. Acum . . . . .                                      | Interference effects in unsteady experiments.<br>Agardograph 109, Chapter IV, AGARD, Paris 1966.  |

TABLE 1

*Comparison of Results for Interference Upwash for  $M=0.7$  at Zero Frequency.*

|                    | Open   |        | Closed |        | Porous slotted |        | Ideal slotted |        | Porous |        |
|--------------------|--------|--------|--------|--------|----------------|--------|---------------|--------|--------|--------|
| $(1+F)^{-1}$       | 1.0    |        | any    |        | 0.811          |        | 0.811         |        | 1.0    |        |
| $(1+\beta/P)^{-1}$ | 1.0    |        | 0      |        | 0.25           |        | 1.0           |        | 0.25   |        |
|                    | A      | B      | A      | B      | A              | B      | A             | B      | A      | B      |
| $\delta_0(M)$      | -0.136 | -0.138 | 0.145  | 0.145  | 0.090          | 0.090  | -0.067        | -0.067 | 0.089  | 0.089  |
| $\delta_1(M)$      | -0.284 | -0.289 | 0.384  | 0.392  | 0.353          | 0.361  | -0.084        | -0.079 | 0.361  | 0.369  |
| $\delta_2(M)$      | 0.000  | 0.010  | -0.001 | +0.010 | 0.166          | 0.174  | -0.001        | +0.010 | 0.167  | 0.175  |
| $\delta_0'(M)$     | 0.114  | 0.114  | -0.050 | -0.049 | -0.038         | -0.037 | 0.081         | 0.081  | -0.040 | -0.039 |
| $\delta_1'(M)$     | 0.137  | 0.136  | -0.145 | -0.141 | -0.191         | -0.189 | 0.067         | 0.067  | -0.197 | -0.195 |
| $\delta_2'(M)$     | 0.006  | -0.002 | 0.014  | 0.029  | -0.042         | -0.027 | 0.005         | 0.008  | -0.029 | -0.014 |

Columns headed A refer to values calculated from equations (15) using incompressible flow results, whilst columns headed B contain results obtained directly from compressible solutions.

TABLE 2

*Interference Parameters for M=0.7.  
Square Tunnel, Closed Side Walls with Various Conditions on Roof and Floor.*

| ROOF & FLOOR            |                            | $\frac{\omega h}{U}$ | $\delta_0$ | $\delta_0'$ | $\delta_1$ | $\delta_1'$ | $\delta_2$ | $\delta_2'$ |
|-------------------------|----------------------------|----------------------|------------|-------------|------------|-------------|------------|-------------|
| $(1+F)^{-1}$            | $(1+\frac{\beta}{P})^{-1}$ |                      |            |             |            |             |            |             |
| CASE 1 (Closed)         |                            |                      |            |             |            |             |            |             |
| any                     | 0                          | 0.01                 | 0.145      | -0.049      | 0.390      | -0.141      | 0.010      | 0.028       |
|                         |                            | 0.5                  | 0.151      | -0.063      | 0.378      | -0.144      | -0.018     | 0.024       |
|                         |                            | 1.0                  | 0.176      | -0.084      | 0.405      | -0.134      | -0.069     | 0.084       |
|                         |                            | 2.0                  | 0.211      | -0.104      | 0.510      | -0.105      | -0.287     | 0.232       |
| CASE 2 (Porous slotted) |                            |                      |            |             |            |             |            |             |
| 0.811                   | 0.25                       | 0.01                 | 0.090      | -0.037      | 0.359      | -0.189      | 0.174      | -0.028      |
|                         |                            | 0.5                  | 0.094      | -0.051      | 0.344      | -0.193      | 0.152      | -0.036      |
|                         |                            | 1.0                  | 0.103      | -0.069      | 0.351      | -0.201      | 0.162      | 0.001       |
|                         |                            | 2.0                  | 0.109      | -0.091      | 0.369      | -0.194      | 0.134      | 0.106       |
| CASE 3 (Porous slotted) |                            |                      |            |             |            |             |            |             |
| 0.811                   | 0.5                        | 0.01                 | 0.023      | 0.007       | 0.234      | -0.156      | 0.276      | -0.144      |
|                         |                            | 0.5                  | 0.024      | 0.004       | 0.207      | -0.136      | 0.225      | -0.112      |
|                         |                            | 1.0                  | 0.027      | 0.004       | 0.168      | -0.109      | 0.210      | -0.108      |
|                         |                            | 2.0                  | 0.057      | -0.028      | 0.114      | -0.127      | 0.085      | -0.092      |
| CASE 4 (Ideal slotted)  |                            |                      |            |             |            |             |            |             |
| 0.811                   | 1.0                        | 0.01                 | -0.067     | 0.081       | -0.079     | 0.067       | 0.010      | 0.009       |
|                         |                            | 0.5                  | -0.055     | 0.067       | -0.077     | 0.060       | 0.007      | -0.005      |
|                         |                            | 1.0                  | -0.032     | 0.055       | -0.061     | 0.051       | 0.013      | -0.022      |
|                         |                            | 2.0                  | 0.036      | 0.032       | -0.031     | 0.046       | -0.069     | -0.057      |
|                         |                            | 3.0                  | 0.142      | -0.007      | 0.122      | 0.088       | -0.642     | 0.032       |
| CASE 5 (Open)           |                            |                      |            |             |            |             |            |             |
| 1.0                     | 1.0                        | 0.01                 | -0.124     | 0.107       | -0.245     | 0.123       | 0.011      | 0.001       |
|                         |                            | 0.5                  | -0.112     | 0.094       | -0.239     | 0.116       | 0.014      | -0.012      |
|                         |                            | 1.0                  | -0.088     | 0.082       | -0.224     | 0.104       | 0.036      | -0.045      |
|                         |                            | 2.0                  | -0.021     | 0.065       | -0.215     | 0.096       | 0.007      | -0.131      |
|                         |                            | 3.0                  | 0.088      | 0.050       | -0.218     | 0.133       | -0.386     | -0.213      |

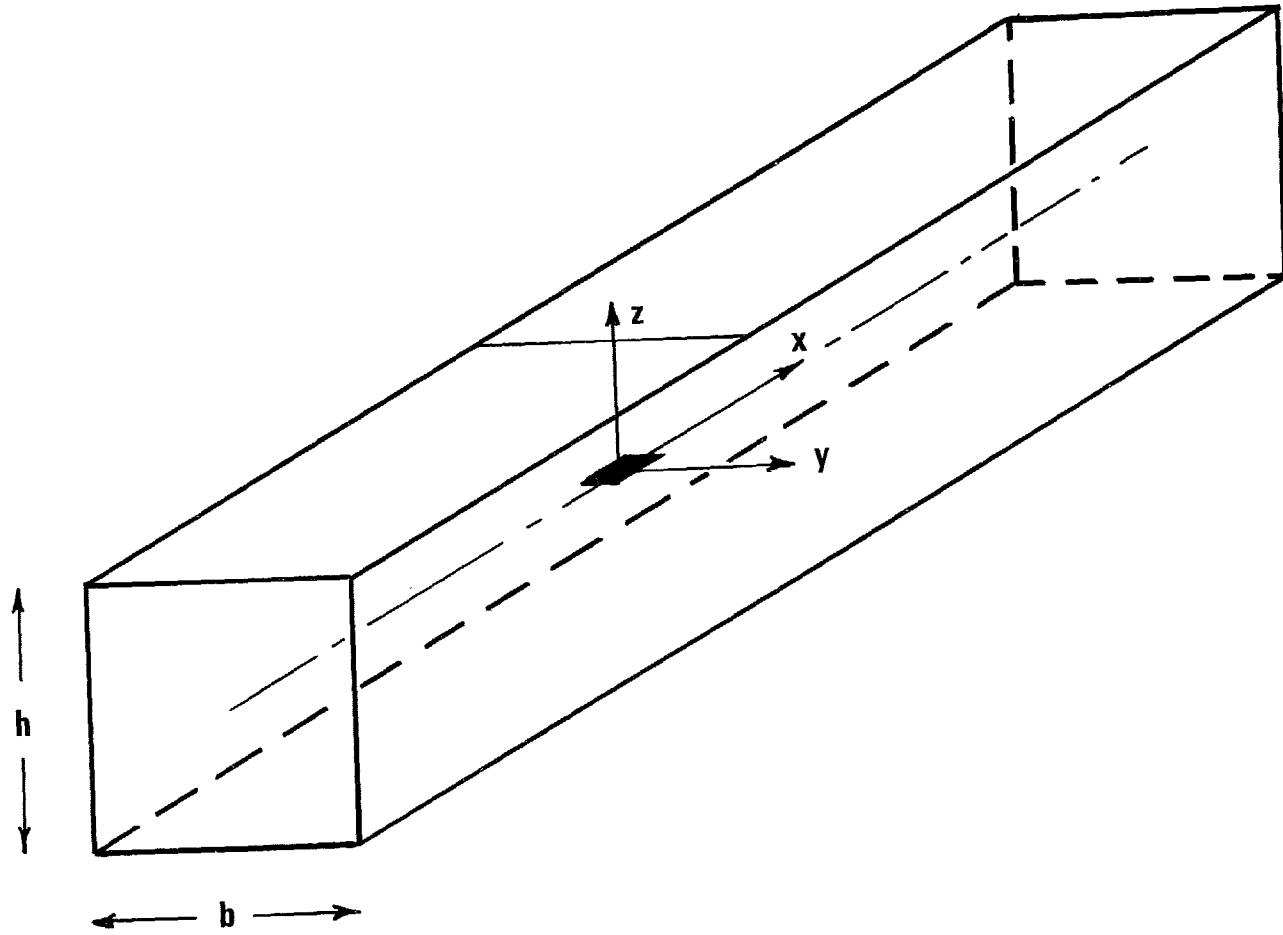


FIG. 1. Co-ordinate system.

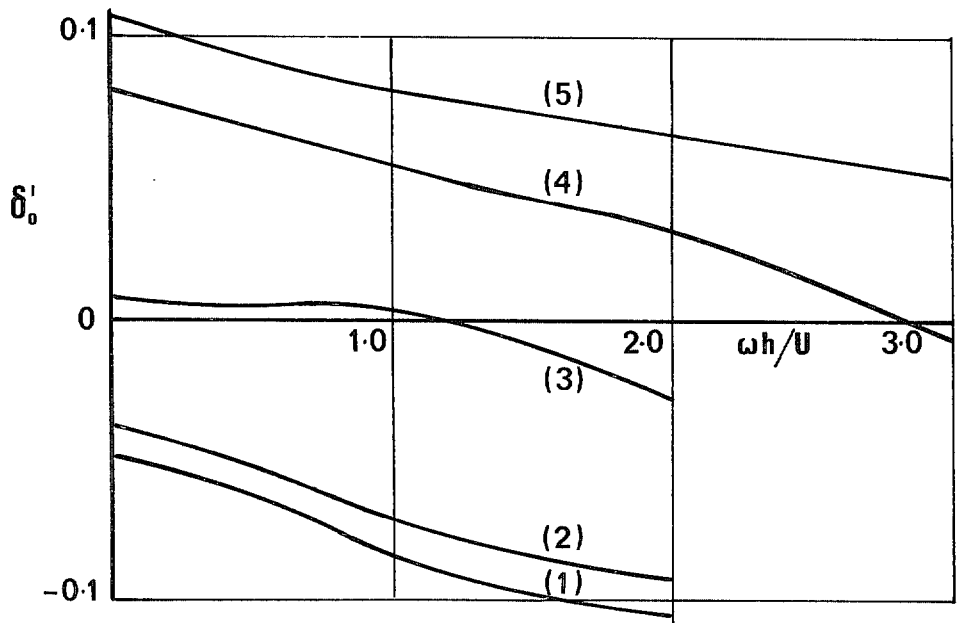
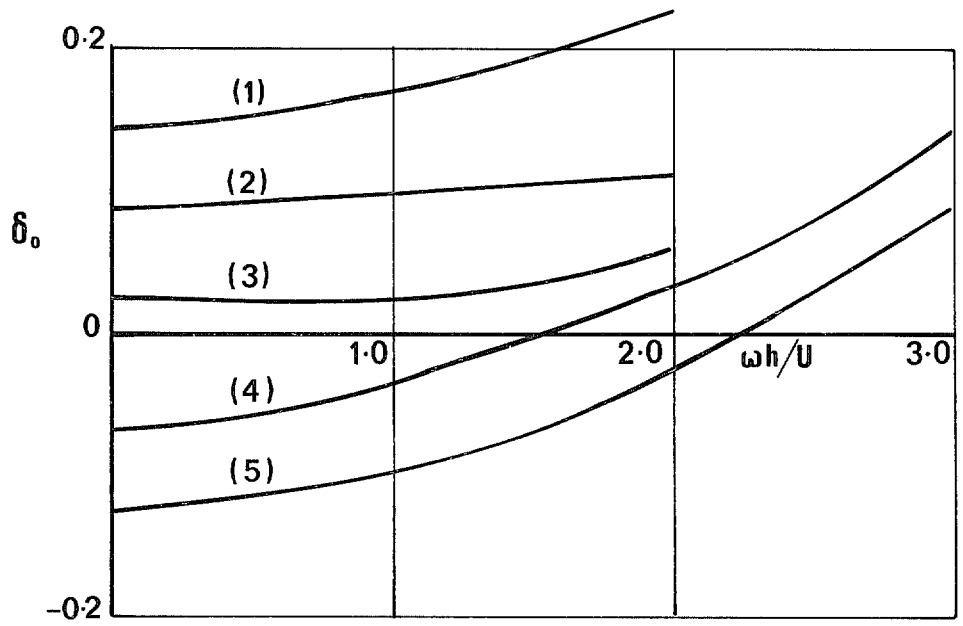


FIG. 2. Variation in  $\delta_0$  and  $\delta'_0$  with frequency,  $M=0.7$ .

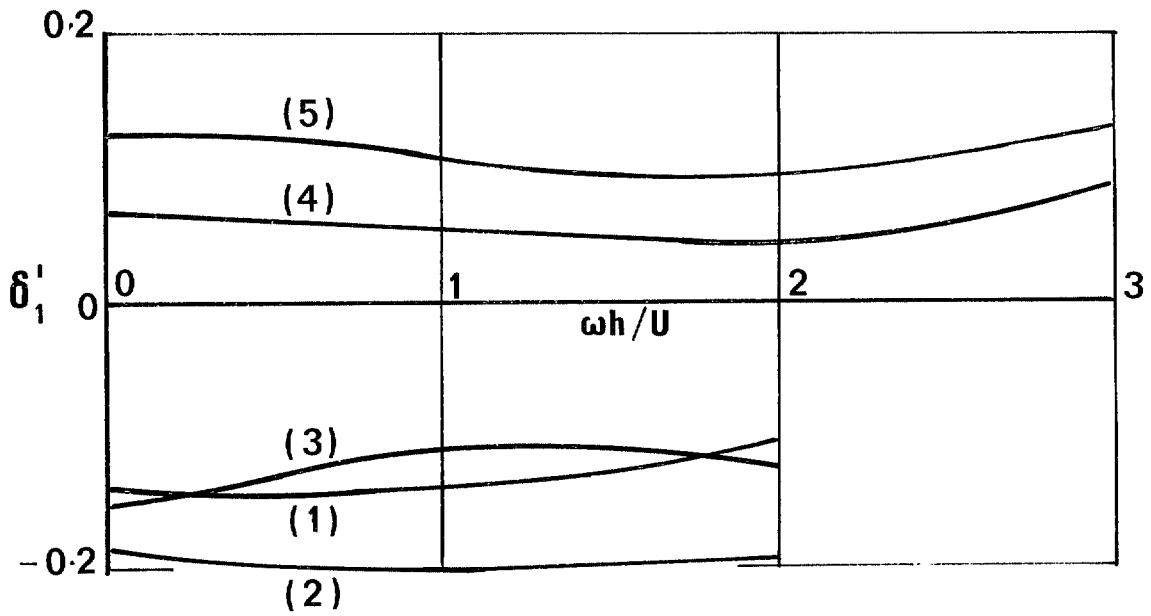
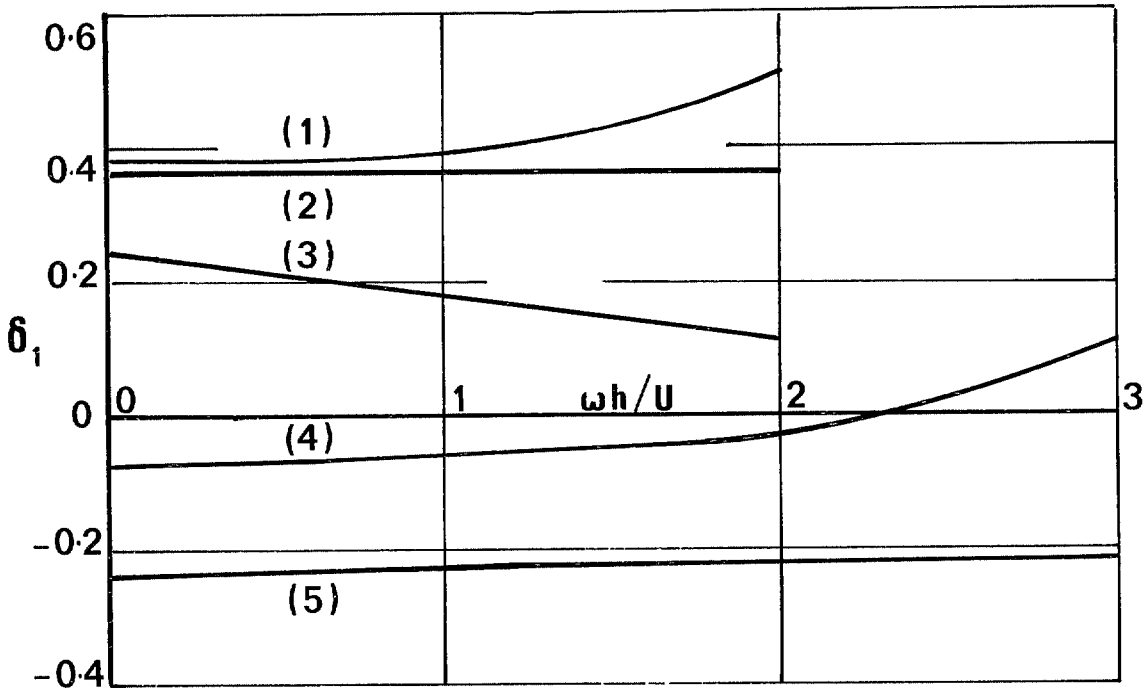


FIG. 3. Variation in  $\delta_1$  and  $\delta'_1$  with frequency,  $M=0.7$ .

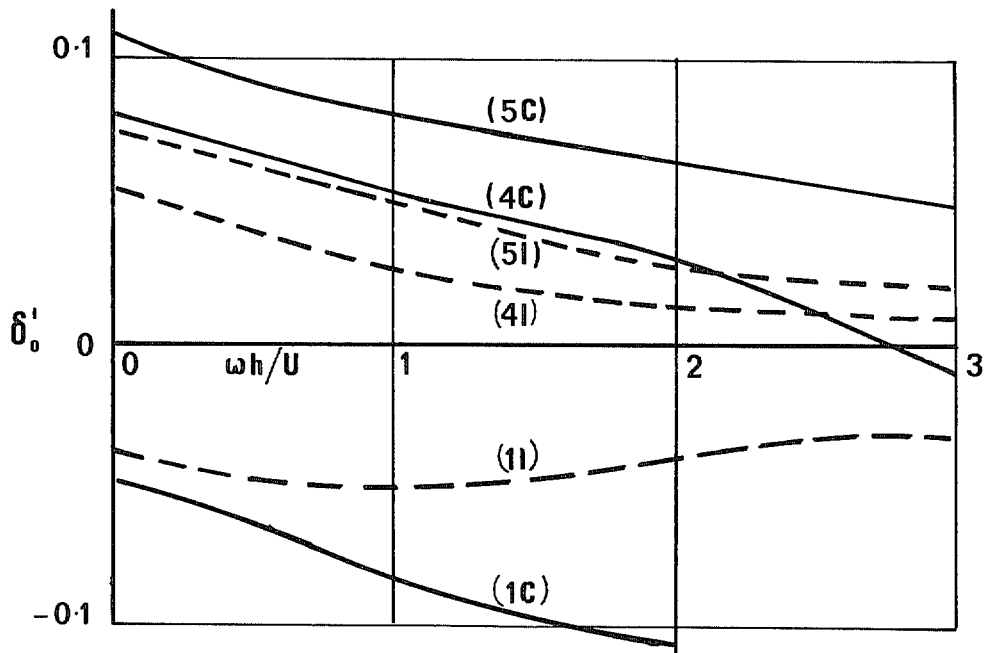
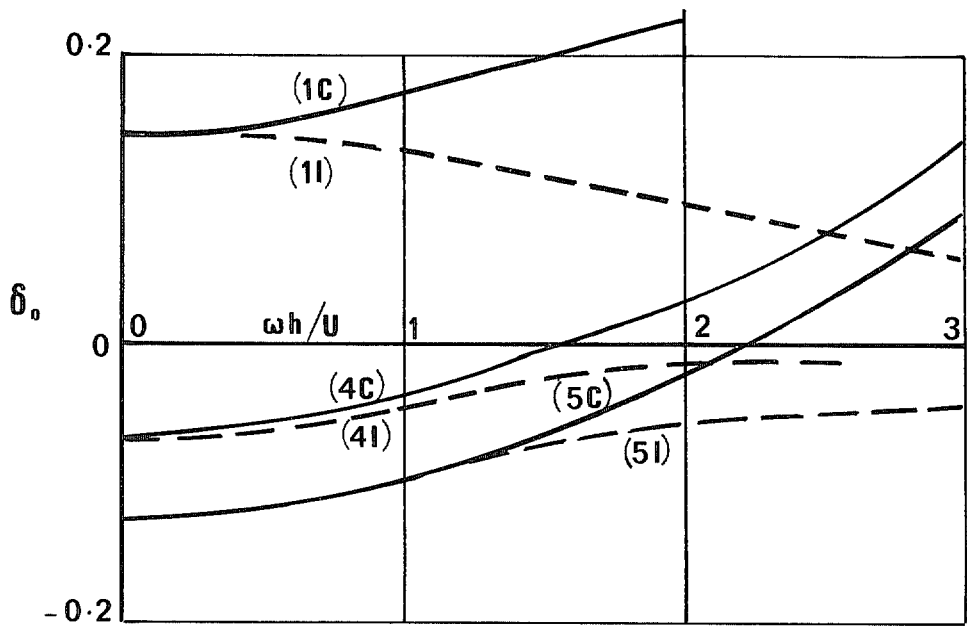


FIG. 4. Variation of interference parameters with frequency. *C* signifies compressible results, *I* incompressible results.

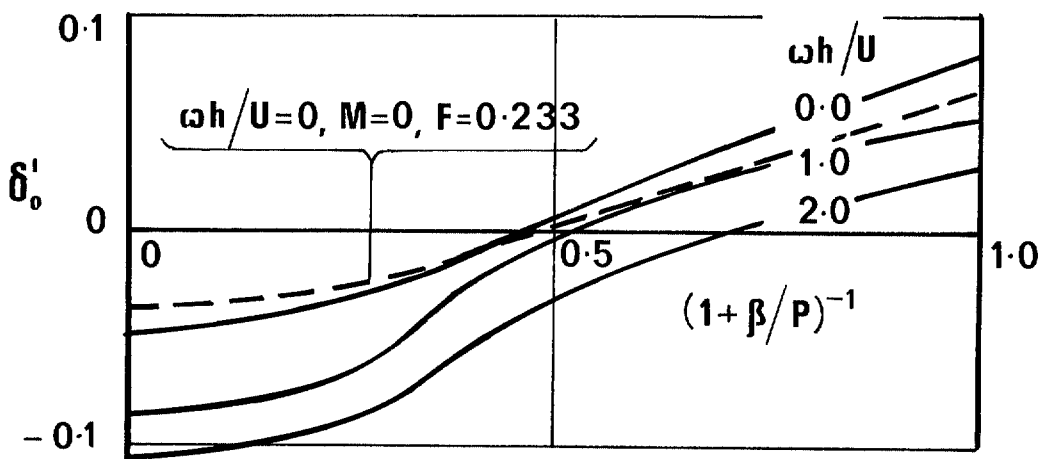
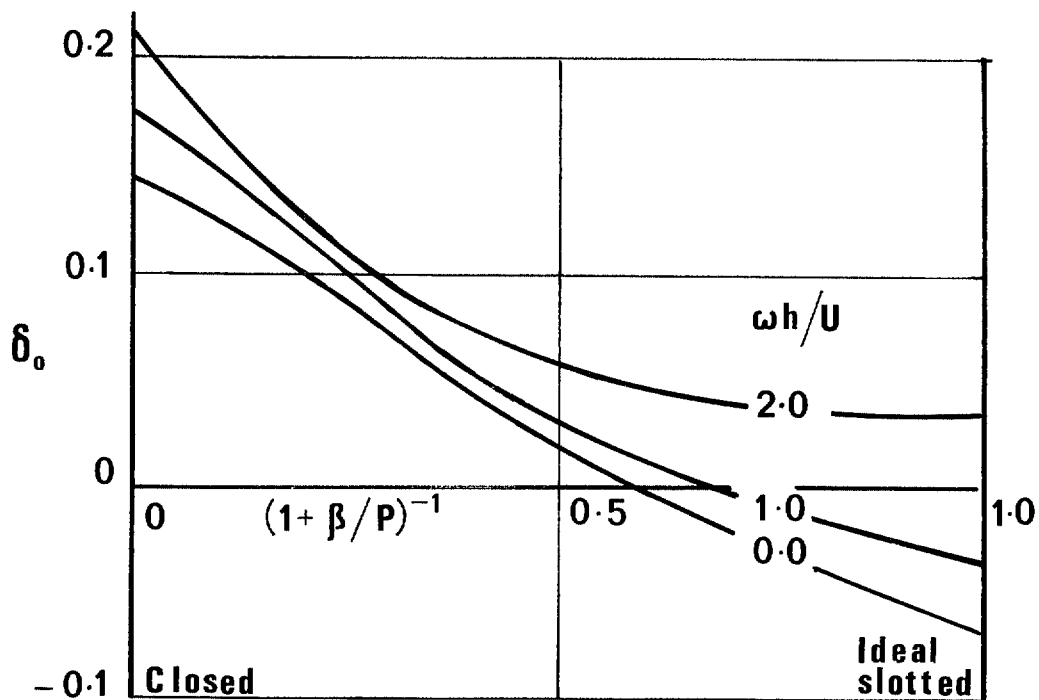


FIG. 5. Variable porosity parameter,  $M=0.7, F=0.233$ . Broken line indicates incompressible result.

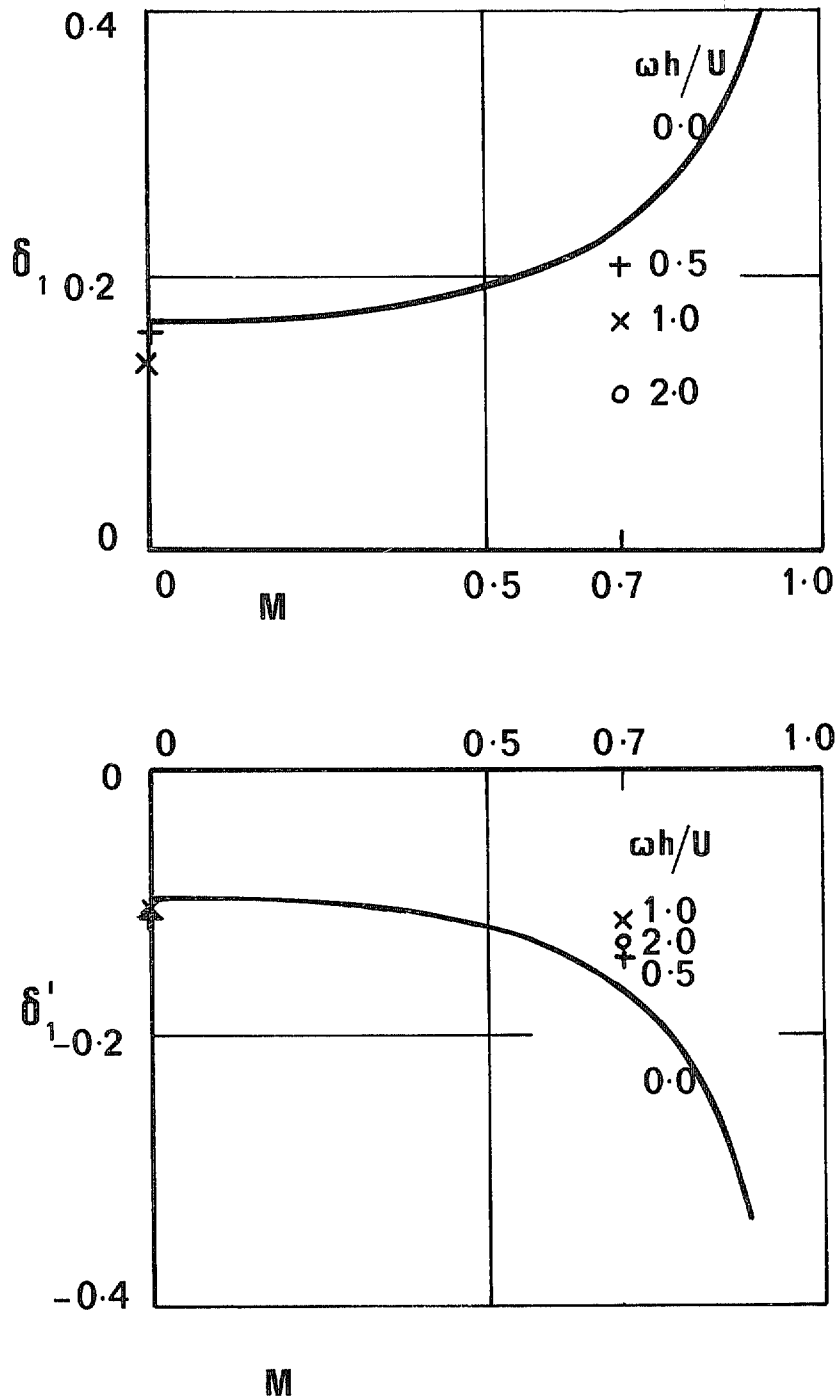


FIG. 6. Effect of Mach number, square tunnel,  $F=0.233$ ,  $\beta/P=1.0$ .

© *Crown copyright* 1972

**HER MAJESTY'S STATIONERY OFFICE**

*Government Bookshops*

49 High Holborn, London WC1V 6HB

13a Castle Street, Edinburgh EH2 3AR

109 St Mary Street, Cardiff CF1 1JW

Brazennose Street, Manchester M60 8AS

50 Fairfax Street, Bristol BS1 3DE

258 Broad Street, Birmingham B1 2HE

80 Chichester Street, Belfast BT1 4JY

*Government publications are also available  
through booksellers*